

**United States Department of the Interior
BUREAU OF RECLAMATION**

**STRESS ANALYSIS
OF HYDRAULIC TURBINE PARTS**

by F. O. Ruud

Denver, Colorado

July 1962

75 cents

United States Department of the Interior

Bureau of Reclamation

Engineering Monographs

No. 30

Stress Analysis
of Hydraulic Turbine Parts

by F. O. Ruud
Engineer, Applied Mathematics and Mechanics Section
Technical Engineering Analysis Branch
Commissioner's Office, Denver, Colorado

Technical Information Branch
Denver Federal Center
Denver, Colorado

CONTENTS

	<u>Page</u>
PREFACE	1
SPIRAL CASE	1
Shell	1
Flange Joints	2
Manholes	2
Man Door	5
STAY RING	6
Ring and Vanes	6
Bolted Joints	9
HEAD COVER	10
Head Cover	10
Attachment to Stay Ring	11
Radial Joints	12
GATE MECHANISM	12
Servomotors	13
Gate Operating Ring	14
Wicket Gate Linkage	14
Wicket Gates	16
SPIRAL CASE SUPPORTING STRUCTURE	17
Jack Loads	17
Tiedown Bars	17
Jack Pads and Tiedown Lugs	17
Support Columns	18
TURBINE RUNNER AND SHAFT	18
Turbine Runner or Pump Impeller	18
Turbine Shaft	19
GUIDE BEARING SUPPORT BRACKET	22
PIT-LINER	23
Collapsing Stability	23
Superimposed Loads	23
Servomotor Supports	24
DRAFT TUBE LINER	24
Collapsing Stability	25
Anchorage	26
Pier Nose	27
Manhole and Man Door	27
MISCELLANEOUS ITEMS	27
Test Bulkheads	27
Bottom Ring	29
LIST OF REFERENCES	31

LIST OF FIGURES

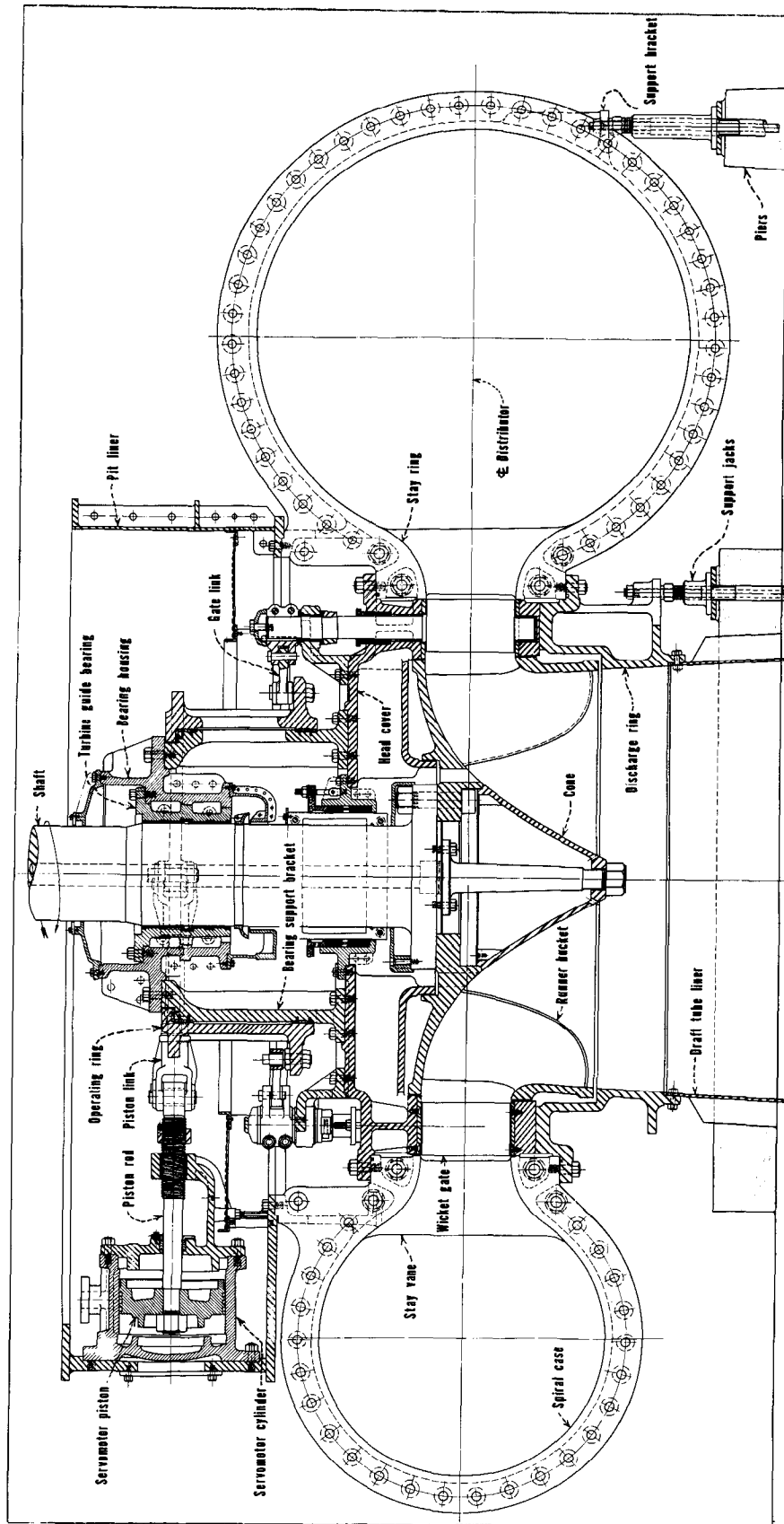
	<u>Page</u>
Frontispiece I Sectional Elevation of Francis Turbine	iv
Frontispiece II Sectional Elevation of Kaplan Turbine	v
<u>Number</u>	
1. Circular Torus	2
2. Elliptical Torus	2
3. Idealization of Man Door Cutout	4
4. Stress Concentration Factors at Manhole	4
5. Two Types of Manhole Reinforcement	5
6. Reinforcing Around Rectangular Manhole	5
7. Stay Vane Cross Section	6
8. Stay Ring Cross Section	8
9. Forces on Stay Ring Bolted Joint	9
10. Section of Head Cover	10
11. Transformed Cross Section of Head Cover.....	12
12. Servomotor Linkage	13
13. Forces on Gate Operating Ring	14
14. Functions of Moment, Shear, and Tension for Ring Solution Shown in Figure 13	15
15. Moments in an Operating Ring	15
16. Gate Linkage Mechanism	16
17. Typical Wicket Gate Linkage System	16
18. Wicket Gate Loads	17
19. Uplift Forces on a Francis Turbine	19
20. Uplift Forces on a Propeller Turbine	19
21. Idealized Shaft Arrangement	20
22. Deflections of Shaft from Inertia Loads	21
23. Unit Load Deflections of Shaft	21
24. Typical Guide Bearing Bracket	22
25. Guide Bearing Bracket	23
26. Servomotor Thrust Plate Loading	24
27. Draft Tube Liner	25

LIST OF FIGURES--Continued

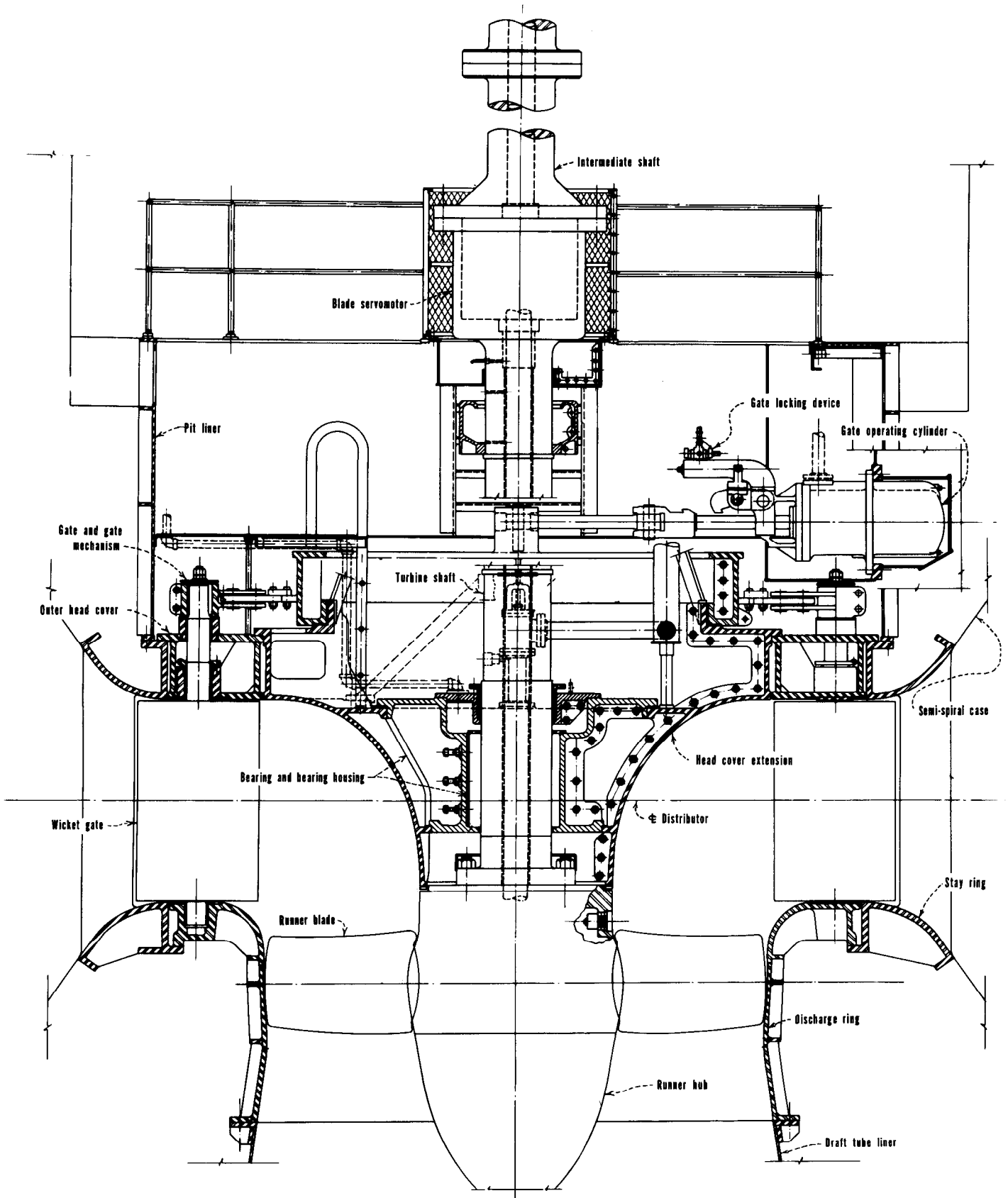
<u>Number</u>		<u>Page</u>
28.	Cast Pier Nose	27
29.	Welded Pier Nose	27
30.	Test Ring	28

LIST OF TABLES

1.	Shell Stresses in the Spiral Case	2
2.	Flange Stresses in the Spiral Case	3
3.	Tabulation of $\psi(\lambda x)$	6
4.	Stay Ring Stress Computation	7
5.	Head Cover Section Properties	11
6.	Computation for Critical Speed.....	20



FRONTISPIECE 1 - Sectional elevation of Francis Turbine.



FRONTISPIECE 2 -Sectional elevation of Kaplan turbine.

PREFACE

This monograph presents procedures for stress analysis of parts for reaction turbines. Many procedures presented herein are also applicable to impulse turbine designs. The procedures have been prepared to assist the engineer with his studies in determining whether a turbine design meets the structural requirements of Bureau of Reclamation Specifications. The methods given are based mainly on mechanics, theory of structures, and strength of materials. They do not include complete elastic-

ity theory solutions, stress concentration allowances, or plastic analyses.

It would be virtually impossible in developing general procedures such as these to provide for all the possible variations which a turbine designer could introduce into his design. Therefore, use of these proposed methods must be based on sound engineering judgment.

The methods of analysis presented in this monograph have been developed over a number of years by engineers of the Bureau's Technical Engineering Analysis Branch. Fundamental contributions to this work were made by F. E. Cornwell, C. C. Crawford, and W. E. Evans.

SPIRAL CASE

The spiral case distributes the flow of water from the penstock around the periphery of the stay ring and into the runner. To maintain a uniform approach velocity of water entering the runner and to supply equal amounts of water to each runner bucket, there is a gradual reduction of area along the length of the spiral case. The cross section of the case may be circular or elliptical, but for purposes of analysis, the cross section at each location is idealized as a continuous torus.

Shell

The design pressure and the maximum allowable stresses for the materials are obtained from the specifications under which the turbine is manufactured and supplied.

For a spiral case of circular cross section, Figure 1, the shell stresses at the point of juncture with the stay ring are computed at every change of thickness of casing or of cross section radius by using the torus formula,¹

$$N_{\phi} = \frac{pa(r_{\phi} + b)}{2 r_{\phi}}$$

where N_{ϕ} = circumferential stress resultant, pounds per inch

p = internal design pressure, pounds per square inch

a = spiral case cross section radius, inches

r_{ϕ} = radius to point of case attachment, inches, (see Figure 8)

b = radius from centerline of unit to center of spiral case cross section, inches

ϕ = angle between vertical and perpendicular to spiral case at r_{ϕ} as shown in Figure 2.

For a spiral case of elliptical cross section, Figure 2, the shell stresses may be computed in a manner similar to that above by using the formula:

$$N_{\phi} = \frac{p(b^2 - r_{\phi}^2)}{2 r_{\phi} \sin \phi}$$

or

$$N_{\phi} = \frac{p(r_{\phi}^2 - b^2)}{2 r_{\phi} \sin \phi},$$

depending upon whether b is greater or less than r_{ϕ} .

¹ S. Timoshenko and S. Woinowsky-Krieger, *Theory of Plates and Shells*, 2nd Ed., 1961, page 441.

TABLE 1 - Shell stresses in the spiral case

JOINT No.	t	a	b	r_ϕ	$(r_\phi + b)$	$\frac{(r_\phi + b)a}{2r_\phi}$	N_ϕ	STRESS, P.S.I.
1								
2								
Etc.								

Note: Make allowance for net area on riveted casings and for joint efficiency factors on welded casings.²

The terms are as defined above and in Figure 2. The shell stress is $\sigma = \frac{N_\phi}{t}$, where t = shell thickness in inches.

Table 1 is used in evaluating the stresses at many points around the spiral case.

Flange Joints

Items to be checked on the spiral case flanges include the following:

a. Radial bending stress in the flange ring.

b. Stress at juncture of hub and flange; this stress is the sum of the bending or discontinuity stress and the direct tension stress due to end pull.

c. Length of hub, if a hub is required, should be approximately equal to $0.611 \sqrt{\frac{Bq_1}{2}}$ (Item 28 on Table 2).

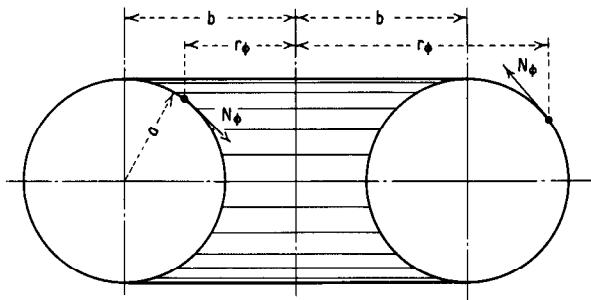


FIGURE 1 - Circular Torus.

d. Tension stress in bolts.

Normally, the flanges on the casing are designed for bearing outside the bolt circle.

² Rules for Construction of Unfired Pressure Vessels, Section VIII, ASME Boiler and Pressure Vessel Code, 1959.

A procedure has been developed for analyzing this type of flange.^{3,4} When several flanges are to be analyzed, which is normally the case, the use of a table will save time and reduce the chance for error. Table 2 and the accompanying figure and notations that define the terms used are recommended.

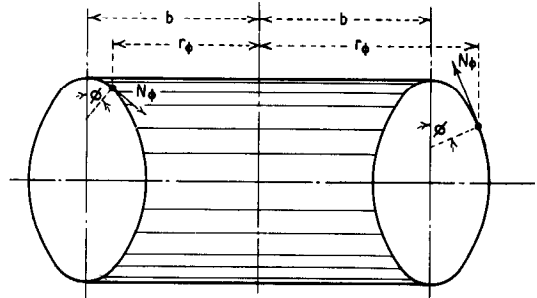


FIGURE 2 - Elliptical Torus.

The flange bolts should be prestressed to not more than twice the working stress or one-half the yield point stress.

Manholes

Manholes in spiral cases are of varying design, but generally are either elliptical or rectangular. They may be cast or fabricated from plate steel sections, and are usually so designed that the normal pressure loading acts to close the man door.

Analytic solutions of the problem of a reinforced circular hole in a flat plate under uniform tension have been prepared.^{5,6}

³ F. E. Cornwell, *Miscellaneous Notes on the General Problem of Flange Design*.

⁴ S. Timoshenko, *Strength of Materials, Part II*, 3rd Ed., 1956, page 141.

⁵ S. Timoshenko and J. N. Goodier, *Theory of Elasticity*, 2nd Ed., 1951, pages 78-85.

⁶ S. Timoshenko, *Strength of Materials, Part II*, 3rd Ed., 1956, page 305.

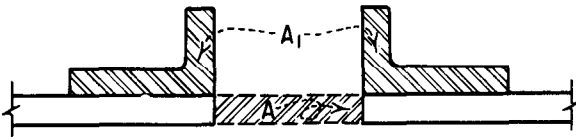


FIGURE 3 - Idealization of manhole cutout.

However, the practical procedure in the analysis of an actual manhole design is necessarily approximate.

Although the membrane forces applied to the man door frame by the shell are well defined, the presence of the opening and its reinforcement causes concentration of stresses. For a circular hole without reinforcement in a flat plate loaded by tension in one direction, the stress concentration factor is 3; for a very rigid circular inclusion the stress concentration factor is 1.5. In addition, the radial loads applied by the man door cause bending stresses in the frame and the surrounding shell. We may conclude that stress concentrations, discontinuity stresses, and bending stresses are always present to some degree. The ultimate test of the design must then be in pressure-proof load.

The following approximate methods may be used as a basis for analysis of man door openings.

The tensile stresses at the manhole, which is normally reinforced, can be determined by referring to Figures 3 and 4.⁶

where A = cross-sectional area of the opening

A_1 = cross-sectional area of the reinforcing material

An approximation, which is true only on the vertical centerline of the spiral case, is to assume the longitudinal tensile stress is one-half the circumferential tensile stress. This would mean that the stress concentration at the edge of the hole instead of being 3 for stress in only one direction would be $(3.0 - 0.5) = 2.5$, when tensions in two mutually perpendicular directions are considered and the value of one stress is one-half the other.⁷

Let

σ = circumferential tension stress without a hole in the casing in pounds per square inch

σ_{max} = the maximum circumferential stress at the edge of the hole in pounds per square inch

Then, Figure 4 gives $\frac{\sigma_{max}}{\sigma}$ versus $\frac{A_1}{A}$. Note that values on the curve apply to stress in one direction only. A correction to σ_{max} thus obtained can be made for a longitudinal stress of $\frac{\sigma}{2}$ by multiplying σ_{max} by $\frac{2.5}{3.0} = 0.833$.

The stress concentration factors above may be used for circular, elliptical (Figure 5), and rectangular (Figure 6) man door openings.⁸ Although the major portion of the reinforcing material should be

⁷S. Timoshenko, *Strength of Materials, Part II*, page 306.

⁸Rules for Construction of Unfired Pressure Vessels, Section VIII, ASME Boiler and Pressure Vessel Code, 1959, Paragraph UG-37.

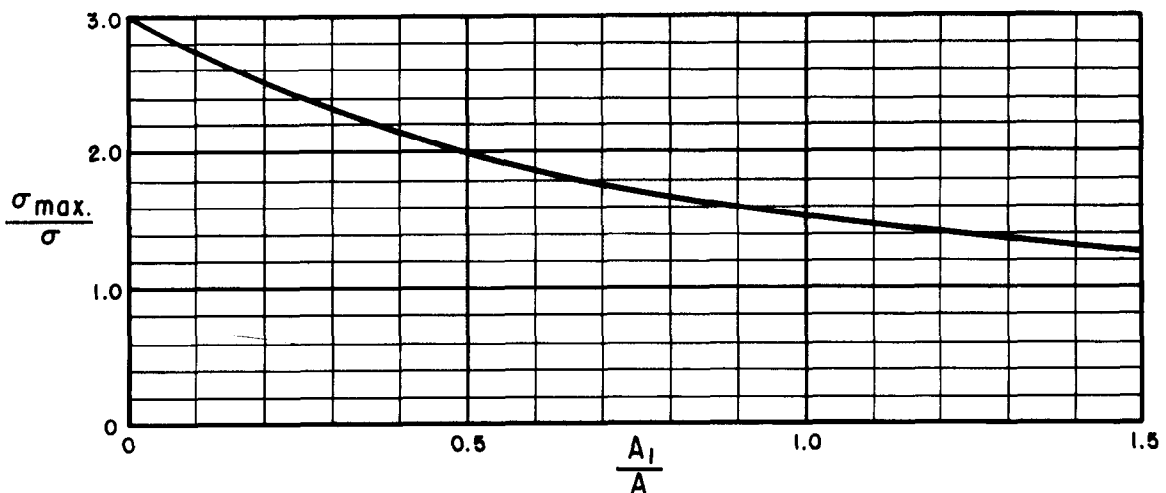


FIGURE 4 - Stress concentration factors at manhole.

at the edge of the opening, some plate reinforcement should be provided around the man door frame to (a) act as a transition between the shell and the man door frame, and (b) to aid in resisting bending of the shell caused by radially directed forces from pressure load on the man door.^{9,10} See References (17) and (18).

Occasionally the methods of Hetenyi¹¹ may be applied to the analysis of the reinforcing plates. When a shear of V pounds per inch is applied to the edge of the spiral casing shell by radial loads on the man door frame, the moment in the shell is

$$M = \frac{V}{2\lambda} e^{-\lambda x} (\cos \lambda x - \sin \lambda x) \quad \text{inch-pounds per inch,}$$

or

$$M = \frac{V}{2\lambda} \psi(\lambda x),$$

where

$$\lambda = \frac{1.285}{\sqrt{at}} \quad (\text{for steel})$$

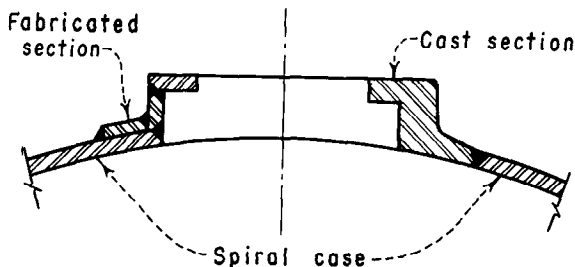


FIGURE 5 - Two types of manhole reinforcement.

x = distance from edge of shell, inches

a = spiral case cross section radius, inches

t = thickness of spiral casing, inches.

Tabulations of $\psi(\lambda x)$ are given in Table 3.

The combined thickness of the plate and shell are required to carry the moment $\frac{V}{2\lambda}$ at the edge of the manhole frame. The

⁹ Mervin B. Hogan, *A Survey of Literature Pertaining to Stress Distribution in the Vicinity of a Hole and the Design of Pressure Vessels*, 1950.

¹⁰ H. Boyd Phillips and Ira E. Allen, *Stresses Around Rectangular Openings in a Plate*, 1960.

¹¹ M. Hetenyi, *Beams on Elastic Foundation*, 1946.

¹² Other formulas for deflection, rotation, and shear of the shell may be found in References (1) and (10).

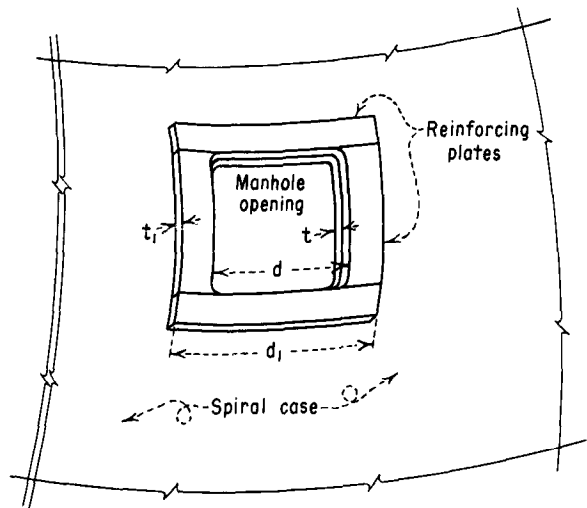


FIGURE 6 - Reinforcing around a rectangular manhole.

thickness of the reinforcing plate should decrease linearly to zero at a distance from the edge of the shell of $\frac{\pi}{4\lambda}$ inches (the first point of zero moment), which is usually adopted as the limit of the reinforcing plates around the opening. The maximum moment which must be carried by the shell beyond this location is approximately $0.2 \left(\frac{V}{2\lambda} \right)$, which is usually acceptable to the shell.

The resistance of the man door frame to the loads applied by the man door should be investigated. Usually the frame is rather rigid and simply transmits these loads through the adjacent plates to the surrounding shell as radial shear forces.

The rectangular man door opening shown in Figure 6 should be provided with generous radii at the corners of the opening to reduce the effects of stress concentration at these points.

Man Door

The man door can be treated as a flat plate reinforced by ribs and subjected to uniform load from the internal pressure in the casing. Consider the edges as simply supported.

An example of a solution for this type of loading is Roark's Case No. 36.¹³ Other solutions are also available.¹⁴ It is noted

¹³ Raymond J. Roark, *Formulas for Stress and Strain*, 3rd Ed., 1954, page 203.

¹⁴ S. Timoshenko and S. Woinowsky-Krieger, *Theory of Plates and Shells*, 2nd Ed., 1961, page 441.

TABLE 3 - Tabulation of $\psi(\lambda x)$

λx	$\psi(\lambda x)$
0	1.00
0.2	0.64
0.4	0.36
0.6	0.14
0.8	-0.01
1.0	-0.11
1.2	-0.17
1.4	-0.20
1.6	-0.21
1.8	-0.20
2.0	-0.18
2.2	-0.15
2.4	-0.13
2.6	-0.10
2.8	-0.08
3.0	-0.06
3.4	-0.02
3.8	-0.004
4.2	0.006
4.6	0.009
5.0	0.008

that the stresses are given for a flat plate. Since the man door is normally a built-up section, it is desirable to determine the moment on the section and consequently the stress. Equating $\frac{6M}{t^2}$ to the expression for stress will give the desired distributed moment, which, when multiplied by the width of the door, may be used in the conventional bending formula to give approximate conservative results.

The tension stress on the root area of the tiedown bolts for the door should also be determined, if applicable, and compared

to the allowable design stress for the bolt material.

STAY RING

The stay ring provides structural continuity between the upper and lower portions of the spiral case, as well as providing passage and guidance for the flow of water to the turbine runner.

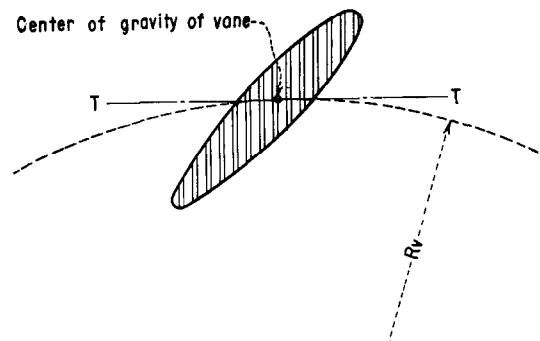


FIGURE 7 - Stay vane cross section.

Ring and Vanes

In the analysis of the stay ring, the procedure given by Evans is followed,¹⁵ Messrs. Bovet can be consulted for additional information.^{16,17}

The moment of inertia of the stay vane cross-sectional area is computed about a tangential axis through its centroid (axis T-T in Figure 7), and the moment of inertia of the stay ring cross-sectional area is computed about a horizontal radial axis through its centroid (axis R-R in Figure 8).

The forces applied to the stay ring are the membrane load of the torus, the pressure on the face of the ring, and the head cover load. Cognizance should be taken of the radial location of load application, as well as the conditions of operation; see Figures 7 and 8 and Table 4.

¹⁵ W. E. Evans, *Stress Analysis of a Hydraulic Turbine Stay Ring*, 1954.

¹⁶ G. and Th. Bovet, *Contribution to the Stress Analysis of a Tubular Scroll*, 1945.

¹⁷ Th. Bovet, *Calculation of the Mechanical Strength of Spiral Casing for High Head Turbines*, 1958.

TABLE 4 - Stay ring stress computation

VANES		OPERATING -- GATES OPEN	
1	p (design pressure, pounds per square inch)		
2	q (tailwater pressure on headcover, pounds per square inch)	43	$\sigma_{TV} = \frac{2 \pi R_V}{n} \cdot \frac{\left[N_V \left(\frac{r_\phi}{R_V} \right) + P_V + P_{C1} \right]}{A_V}$
3	θ (location of stay vane from inlet)		
4	θ_2 (angle of shell load resultant)	44	$M_{R0} = M_{R1} + M_{R2} + M_{R3} + M_{R4} + M_{R5-1}$
5	n (number of stay vanes for spacing)	45	$M_{V0} = \frac{M_{R0} 2 \pi R_V (1-\lambda)}{n}$
6	a (spiral casing radius, inches)		
7	b (radius to torus centerline, inches)	46	$\sigma_{bv} = \frac{M_{V0} C_V}{I_T}$
8	r_0 (radius to shell attachment, inches)	47	$\sigma_{Total} = \sigma_{TV} + \sigma_{bv}$
9	L (height of stay vane at R_V , inches)		
10	R_g (radius to ring center of gravity, inches)	OPERATING -- GATES CLOSED	
11	R_b (runner seal radius, inches)		
12	R_c (headcover seal radius, inches)	48	$\sigma_{TV} = \frac{2 \pi R_V}{n} \cdot \frac{\left[N_V \left(\frac{r_\phi}{R_V} \right) + P_V + P_{C2} \right]}{A_V}$
13	R_d (headcover bolt circle radius, inches)	49	$M_{RC} = M_{R1} + M_{R2} + M_{R3} + M_{R4} + M_{R5-2}$
14	R_g (wicket gate circle radius, inches)	50	$M_{VC} = \frac{M_{RC} 2 \pi R_V (1-\lambda)}{n}$
15	R_s (shaft seal radius, inches)	51	$\sigma_{bv} = \frac{M_{VC} C_V}{I_T}$
16	R_V (radius to stay vane center of gravity, inches)	52	$\sigma_{Total} = \sigma_{TV} + \sigma_{bv}$
17	Y_r (vertical location of ring centroid, inches)		
18	Y_s (vertical location of outer edge of shell at r_0 , inches)	TEST -- (p' = test pressure)	
19	$Y_\phi = Y_s + \frac{1}{2} \cos \theta_2$ (vertical location of shell centerline at r_ϕ , inches)		
20	$Y_v = \frac{1}{2}$ (vertical location of horizontal pressure load P_H , inches)	53	$\sigma_{TV} = \frac{2 \pi R_V}{n} \cdot \frac{\left[N_V \left(\frac{r_\phi}{R_V} \right) + P_V \right]}{A_V} \cdot \frac{p'}{p}$
21	$R_H = \frac{2}{3} \left(\frac{r_0^3 - R_c^3}{r_0^2 - R_c^2} \right)$ (radius to center of gravity of vertical pressure load on element of ring, inches)	54	$M_{RT} = M_{R1} + M_{R2} + M_{R3} + M_{R4}$
22	$r_\phi = r_0 - \frac{1}{2} \sin \theta_2$ (radius to centerline of shell attachment, inches)	55	$M_{VT} = \frac{M_{RT} 2 \pi R_V (1-\lambda)}{n}$
23	C_V (radial distance from vane centroid to extreme tension fiber, inches)	56	$\sigma_{bv} = \frac{M_{VT} C_V}{I_T} \cdot \frac{p'}{p}$
24	A_R (area of ring cross-section, inches ²)	57	$\sigma_{Total} = \sigma_{TV} + \sigma_{bv}$
25	A_V (area of stay vane cross-section, inches ²)	RING	
26	I_R (moment of inertia of ring area about axis RR, inches ⁴)	58	$\lambda M_{RC} = M_{SR}$
27	I_T (moment of inertia of vane area about axis TT, inches ⁴)	59	$\Sigma H = N_H \frac{r_\phi}{R_V} - P_H$ (use maximum value of ΣH)
28	t (thickness of spiral case shell, inches)	60	$\Sigma V = N_V \frac{r_\phi}{R_0} + (P_V + P_{C2}) \cdot \frac{R_V}{R_0}$
29	$N_\phi = p a \cdot \frac{(r_\phi + b)}{2 r_\phi}$ (spiral case circumferential stress resultant, pounds per inch, at radius r_ϕ)	61	$M_s = \frac{\Sigma V}{12} \left(\frac{2 \pi R_q}{n} \right)^2$
30	$N_V = N_\phi \sin \theta_2$ (vertical component of N_ϕ)	62	$M_{SR} R_V$
31	$N_H = N_\phi \cos \theta_2$ (horizontal component of N_ϕ)	63	$\sigma_{TR} = \frac{\Sigma H R_V}{A_R}$
32	$P_V = p \cdot \frac{(r_0^2 - R_c^2)}{2 R_V} - \frac{p A_V n}{2 \pi R_V}$ (vertical pressure load on ring element, pounds per inch, at radius R_V)	64	$\sigma_{br} = \frac{M_s + M_{SR} R_V}{I_R} Y_r$
33	$P_H = p Y_s \cdot \frac{(r_0 + R_c)}{2 R_V}$ (horizontal pressure load on ring element, pounds per inch, at radius R_V)	65	$\sigma_{Total} = \sigma_{br} + \sigma_{TR}$
34	$P_{C1} = \frac{p (R_c^2 - R_g^2) + 0.7 p (R_g^2 - R_b^2) + q (R_b^2 - R_s^2)}{2 R_V}$ (headcover load, gates open, pounds per inch at R_V)	BOLTED JOINTS	
35	$P_{C2} = p \cdot \frac{(R_c^2 - R_g^2)}{2 R_V}$ (headcover load, gates closed, pounds per inch at radius R_V)	66	A_F (area of flange face)
36	$M_{R1} = N_V (r_\phi - R_V) \frac{r_\phi}{R_V}$	67	Y_F (vertical location of face centroid)
37	$M_{R2} = N_H (Y_r - Y_\phi) \frac{r_\phi}{R_V}$	68	A_b (area of bolts)
38	$M_{R3} = P_H (Y_v - Y_r)$	69	Y_b (vertical location of bolts' centroid)
39	$M_{R4} = P_V (R_H - R_V)$	70	I_F (moment of inertia of flange face area)
40	$M_{R5-1} = P_{C1} (R_d - R_V)$	71	$T = \Sigma H R_V$
41	$M_{R5-2} = P_{C2} (R_d - R_V)$	72	$(Y_F - Y_r)$
42	$\lambda = \frac{M_{SR}}{M_R} = \frac{\pi R_V I_R L}{R_V R_0 I_T n + \pi R_V I_R L}$ (part of total twisting moment carried by ring)	73	$(Y_b - Y_f)$
		74	$\sigma = \frac{T - B}{A_F} + \frac{T(Y_F - Y_r) + B(Y_b - Y_f) + M_{SR} R_V}{I_F} Y_f \leq 0$
		75	B (required preload of bolts)
		76	$\sigma_{bolts} = \frac{B}{A_b}$

Since the radial forces on the stay ring are resisted by tension in the ring, and the vertical forces are resisted by tension in the vanes, the total applied twisting moment M_R is found by summation of moments of the radial forces about a tangential axis through the ring centroid and the moments of the vertical forces about a tangential axis through the centroid of the vane. M_R is then divided between the ring and the vane in proportion to their relative stiffnesses, as follows:

$$M_{SR} = \lambda M_R,$$

where M_{SR} is the twisting moment on the ring, inch-pounds per inch at R_v , and

$$\lambda = \frac{\pi R_v I_R L}{R_v R_a I_T n + \pi R_v I_R L}$$

R_v = radius to centroid of vane, inches

I_R = moment of inertia of ring, inches⁴

L = height of vane at centroid, inches

R_a = radius to centroid of ring, inches

I_T = moment of inertia of vane, inches⁴

n = number of vanes (assume equally spaced).

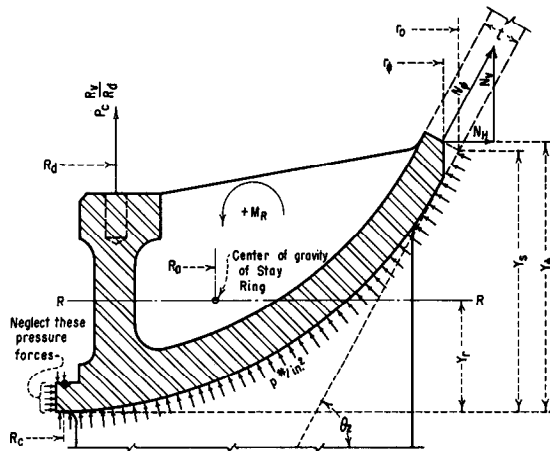


FIGURE 8 - Stay ring cross section.

Then

$$M_v = \frac{M_R 2\pi R_v (1 - \lambda)}{n},$$

where M_v is bending moment on the stay vane in inch-pounds.

Stresses in the ring and the vane may then be computed as follows:

$$\sigma_{ring} = \frac{\Sigma H R_v}{A_R} + \frac{M_S + M_{SR} R_v}{I_R} Y_T, \text{ pounds}$$

per square inch

where

A_R = cross-sectional area of stay ring, square inches

M_S = bending moment in a vertical plane of stay ring at the support, inch-pounds

Y_T = vertical location of ring centroid, inches

ΣH = sum of horizontal forces acting on stay ring (pounds per inch at R_v), pounds per inch

and

$$M_S = \frac{\Sigma V}{12} \left(\frac{2\pi R_a}{n} \right)^2,$$

using

$$\Sigma V = N_v \frac{r_{\phi}}{R_a} + (P_v + P_{c2}) \frac{R_v}{R_a},$$

pounds per inch at R_a .

Also,

$$\sigma_{vane} = \frac{\Sigma V 2\pi R_v}{n A_v} + \frac{M_v}{I_T} c_v, \text{ pounds per}$$

square inch,

where

ΣV = sum of vertical forces acting on stay vane (load per inch at R_v), pounds per inch

A_v = cross-sectional area of stay vane, square inches

I_T = moment of inertia of vane area about a tangential axis through centroid, inches⁴

c_v = radial distance from vane centroid to extreme tension fiber, inches.

Table 4 is recommended for use in computing the stresses.

An approximate check computation for the stay vane stresses may be obtained with the following formula:

$$\sigma = p \frac{2\pi R_v}{n} \left[\frac{2ab - a^2}{2b - 2a} \left(\frac{b - a - R_v}{I_T} c_v + \frac{1}{A_v} \right) + \frac{b - a - R_v}{A_v} \right]$$

where

p = spiral case internal pressure, pounds per square inch

a = spiral casing radius, inches

b = radius to torus centerline, inches

I_T = moment of inertia of stay vane about tangential axis through center of gravity, inches⁴, (see Figure 7).

This formula applies the torus shell stress resultant to the stay vanes eccentrically, at the horizontal centerline of the spiral case.

Bolted Joints

Bolted joints occur in nearly all stay rings and must be designed to resist the most severe conditions of loading which may be applied.

The following comments generally apply to all stay ring bolted joints:

a. The bolts should be prestressed to not more than twice the maximum applied working stress, or 50 percent of the yield point stress.

b. The thickness of the flanges should be at least 1-1/2 times the maximum bolt diameter.

c. The externally applied loading should combine the effects of eccentrically applied tension and moment at the location of the bolted joint.¹⁸

¹⁸T. J. Dolan, and J. H. McClow, *The Influence of Bolt Tension and Eccentric Loads on the Behavior of a Bolted Joint*, 1950.

d. The required preload of the bolts on the joint face (bolt stress multiplied by bolt area) must prevent the joint from opening under any condition of applied loading.

At point '0' of Figure 9, the joint must not open. Therefore, assuming rigid flange faces,

$$0 \geq \frac{T - B}{A_F} + \frac{T(Y_F - Y_R) + B(Y_b - Y_F) + M_{SR} R_v}{I_F} Y_F$$

where

A_F = area of flange face, square inches

I_F = moment of inertia of flange face area about a horizontal centroidal axis, inches⁴

Y_F = distance from bottom edge of stay ring to centroidal axis, inches

Y_b = distance from bottom edge of stay ring to centroid of bolt pattern, inches

Y_R = distance from bottom edge of stay ring to centerline of application of tensile load, inches

B = total bolt force, pounds

T = total tensile force, pounds

$M_{SR} R_v$ = total applied moment, inch-pounds.

The use of Table 4 will facilitate the computing process.

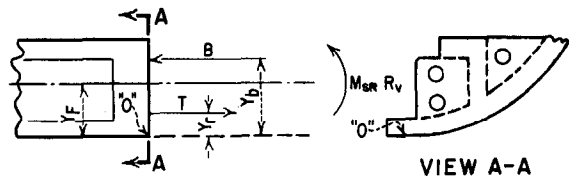


FIGURE 9 - Forces on stay ring bolted joint.

HEAD COVER

The head cover is used to seal off the region above the turbine runner and to direct the flow down through the runner. It is bolted to the stay ring. Usually, the lower main shaft guide bearing and packing box are supported on the head cover. There is a watertight seal between the head cover and the stay ring, and there is a wearing ring between the head cover and the runner.

Unless the head cover load is specified, it will be assumed that design pressure acts on the annular area of the head cover between the stay ring seal and the wearing ring.

Figure 10 shows a cross-sectional view of a head cover. The sections shown are only those which are continuous around the circumference of the cover.

Head Cover

To compute tangential stresses in the head cover, it is analyzed as a circular ring whose width is not small compared to its radius, subjected to twisting moments distributed along its centerline ¹⁹

The tangential stress at the location y, r (see Figure 10), is given by:

$$\sigma = \frac{My}{r} \frac{1}{\iint \frac{y^2}{r} dr dy}$$

$$M = \frac{L}{2\pi} \left[R_d - \frac{2(R_c^3 - R_b^3)}{3(R_c^2 - R_b^2)} \right]$$

$$L = p\pi(R_c^2 - R_b^2)$$

where

σ = the tangential stress, pounds per square inch

M = the total bending moment on any radial cross section of the head cover, inch-pounds

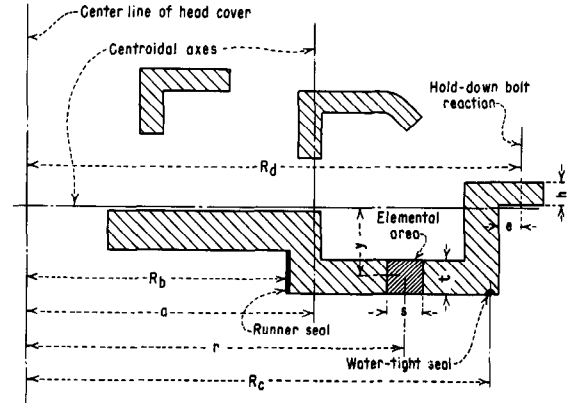


FIGURE 10 - Section of head cover.

y = the distance from the horizontal centroidal axis of the head cover cross section, inches (positive when measured upward)

r = the distance from the center of the head cover to the point under consideration, inches

L = the total hydrostatic load on the head cover, pounds

R_d = the radius of the head cover holddown bolt circle, inches

R_c = the radius to the head cover stay ring seal, inches

R_b = the radius to the runner seal inches

p = the hydrostatic pressure, pounds per square inch

Integration of the expression $\iint \frac{y^2}{r} dr dy$ is effected by dividing the cross-section shown in Figure 10 into a suitable number of elemental areas. The following expression gives the contribution of the individual element to the moment of inertia of the section:

$$\frac{Ay^2 + \frac{St^3}{12}}{r}$$

where

A = the area of the element, square inches

¹⁹S. Timoshenko, *Strength of Materials, Part II*, 3rd Ed., 1956, page 140.

S = the length of a rectangular element in the r-direction, inches

t = the length of a rectangular element in the y-direction, inches

The summation as shown in Table 5 will give a good approximation to the value of the double integral.

The maximum tangential stress in the head cover can be computed from the expression previously stated.

$$\sigma = \frac{My}{r} \frac{1}{\iint \frac{y^2}{r} dr dy}$$

using the location in the cross section where the ratio y/r is maximum. This location is usually at the inside edge of the head cover and may be at the top or bottom.

Attachment to Stay Ring

The head cover is usually attached to the stay ring by bolts through a flange at the outer edge of the cover. To check this connection, two computations will usually suffice. The tensile stresses should be computed at the root areas of the bolts; also, the bending stresses should be computed in the flange, acting as a cantilever beam.

The bolt stress is given by:

$$\sigma_b = \frac{L}{nA_b}$$

where

σ_b = the bolt stress, pounds per square inch

n = the total number of bolts holding the head cover to the stay ring

A_b = the net area of one bolt at the thread root, square inches

L = the total hydrostatic load on the head cover, pounds.

The bending stress in the holddown flange is given by:

$$\sigma = \frac{pe(R_c^2 - R_b^2)}{R_d h^2} \quad \text{or} \quad \sigma = \frac{3eL}{\pi R_d h^2}$$

where

σ = the bending stress in the holddown flange, pounds per square inch

p = the hydrostatic pressure, pounds per square inch

e, R_c , R_b , R_d , and h are dimensions in inches as shown in Figure 10.

The above bolt stress and the bending stress in the holddown flange are based on

TABLE 5 - Head cover section properties

ELEMENT	s	t	A	y	r	$\frac{Ay^2}{r}$	$\frac{st^3}{12r}$
1							
2							
3							
i							
						$i \sum \left(\frac{Ay^2}{r} + \frac{st^3}{12r} \right) =$	

an assumed direct bolt pull with no flange action. This condition is considered unconservative for the bolt stress and overly conservative for the flange bending stress. An assumed complete restraint (against rotation) at the bolt circle would reduce the flange bending stress to one-half the value computed above. The increased bolt pull or stress with flange action can be obtained by multiplying the stress computed above by the lever arm ratio:

$$\frac{\text{flange O.D.} - 2R_d + e}{\text{flange O.D.} - 2R_d}$$

The actual flange and bolt stresses are probably between the two extremes computed above, but somewhat nearer to the latter case.

In addition to the bolting there is a dowel requirement between the head cover and stay ring. If the operating ring is guided by the bearing support bracket, it is smaller in diameter than the wicket gate circle. For this case, if one of the servomotor pistons is against its stop, a horizontal thrust of double the thrust of the individual servomotor is applied to the bearing bracket (assuming that the lines of thrust from the two servomotors are parallel). This load is then transferred to the head cover (normally by dowels from the bearing bracket to the head cover, but in some instances by bearing contact) and from the head cover to the stay ring. Neglecting frictional resistance to sliding of the head cover on the stay ring, adequate dowels should be provided to carry the horizontal thrust computed on the above basis.

If the operating ring is guided by the pit liner or is in such position that the lateral thrust is not resisted by the bearing bracket and head cover, then the dowels between the head cover and stay ring should be designed to resist the loads from the maximum servomotor torque.

In arriving at the dowel requirement, it is considered realistic to use a working shear stress in steel dowels of 15,000 pounds per square inch, since frictional resistance to sliding of the head cover on the stay ring is neglected.

Radial Joints

The bolts holding the sections of the head cover together should be checked for strength. The total bending moment on any radial cross section of the head cover is given by the formula,

$$M = \frac{L}{2\pi} \left[R_d - \frac{2(R_c^3 - R_b^3)}{3(R_c^2 - R_b^2)} \right]$$

After M is computed, the tensile stress in the bolts can be computed from the formula:

$$\sigma_b = \frac{My}{I}$$

where

σ_b = the stress in the bolts holding the sections of the head cover together, pounds per square inch

M = as above, inch pounds

y = the distance from the neutral axis of the transformed cross section of the head cover to the bolt under consideration, inches, see Figure 11

I = the moment of inertia of the transformed cross section of the head cover, inches⁴, see Figure 11.

The bolts should be prestressed to not more than twice the working stress or one-half the yield point stress.

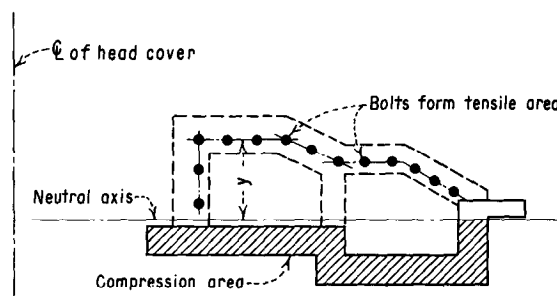


FIGURE 11 - Transformed cross section of head cover.

GATE MECHANISM

The gate mechanism consists of the servomotor, the operating ring, the gate linkage, and the wicket gates. The gate mechanism transmits the force and movement

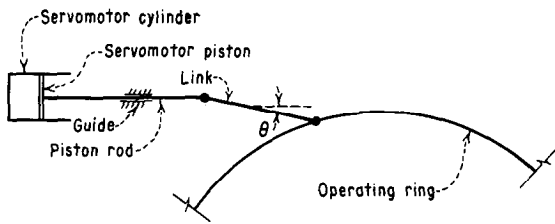


FIGURE 12 - Servomotor linkage.

of the servomotor piston to the wicket gates in regulating flow of water to the turbine runner.

Servomotors

The function of the servomotor is to supply the force necessary to operate the wicket gates. The maximum oil pressure is applied to the piston, and the maximum stresses are then determined in the piston, the piston rod, the cylinder wall, the cylinder head and head bolts, and the flange and flange bolts holding the servomotor to the pit liner. (See the section on attachment to stay ring.)

In the connections between the servomotor piston rod and the link, and between the link and the operating ring, the shear stress in the pin and the tear-out of the link end should be checked.

The anchorage of the servomotor through the pit liner into the foundation concrete should be adequate to hold the full tension force of the servomotor. This is usually accomplished by rods extending into the concrete with anchor plates at their ends. An analysis of the servomotor backup plate will be found in the section on pit liners.

Consider the relative lengths of the servomotor piston rod and the servomotor link, Figure 12. Since the connection of the link to the operating ring must follow a circular path, although only for a short distance, this point will move laterally with respect to the servomotor piston rod centerline. This movement will cause the link force to act at an angle θ to the piston rod centerline and to induce a lateral force applied at the end of the piston rod.

Typical installations show the link to be approximately the same length as the piston rod. If the link is relatively long, this lateral force will be small, since the angle θ is small. However, if the link is short, the force may be large, because a relatively large angle may be formed for a given lateral displacement.

When the lateral displacement of the end of the link is small (so that small angle functions apply), the friction forces in the pins are no longer negligible. These may be considered by the use of friction circles. The radius of the friction circle is:

$$r = \mu R$$

where

μ = coefficient of friction in the joint (may vary from 0.05 to 0.15)

R = pin radius, inches.

The resulting line of action of the link is tangential to the friction circles and acts in such a direction as to oppose the motion.

For small angles, this may result in much smaller deflections of the piston rod than when friction is neglected. (Note that the initial lateral displacement is affected by the clearance between the piston and cylinder and the piston rod and guide sleeves.)

Since the thrust of the servomotor is given, the lateral load on the piston rod can be calculated by multiplying the servomotor thrust by $\tan \theta$. θ should be the largest possible angle that the link makes with the piston rod. To check for safe working stresses, the following formula may be applied: (See page 7 of Timoshenko's work on the theory of elastic stability.)

$$\sigma = \frac{Mc}{I} + \frac{P}{A}$$

where

P = servomotor thrust

$$M = Pk \tan \theta \tan \frac{L}{k}$$

$$k = \sqrt{\frac{EI}{P}}$$

The stress in the piston rod should not exceed the yield point stress divided by a suitable factor of safety. If the angle θ is negligible, the stress should not exceed:

$$\text{For } \frac{L}{r} < 60 \quad \frac{P}{A} = 10,000 \text{ psi}$$

$$\text{For } \frac{L}{r} > 60 \quad \frac{P}{A} = \frac{18,000}{1 + \frac{4}{18,000} \left(\frac{L}{r} \right)^2}$$

where

- L = length of piston rod acting as a cantilever beam, inches
- r = minimum radius of gyration of the piston rod cross section, inches
- A = cross section area of piston rod, square inches
- P = servomotor thrust, pounds
- M = maximum moment caused by the servomotor thrust, inch-pounds
- E = modulus of elasticity, pounds per square inch
- I = moment of inertia of piston rod, inches⁴
- θ = acute angle that piston rod makes with link, see Figure 12.

Deflection of the end of the piston rod can be checked by the following formula:²⁰

$$y = \left(\sqrt{\frac{EI}{P}} \tan \frac{L}{\sqrt{\frac{EI}{P}}} - L \right) \tan \theta$$

Gate Operating Ring

The function of the gate operating ring is to distribute the thrust from the servomotors to the individual wicket gate linkages.

The operating ring may be considered as a ring acted upon by a couple consisting of servomotor forces applied to the ring at the link connections and resisted by the distributed reactions of the gate linkage connections. See Figure 13.

A number of ring solutions applicable to various problems may be found;²¹ others have been solved for special cases (see Figure 15). However, most actual analyses may require superimposing two or more simple solutions.

Stresses in the operating ring are limited by the maximum servomotor thrust, and are:

$$S = \frac{Mc}{I} + \frac{T_1}{A} + \frac{T_2}{A}$$

where

- P = maximum servomotor thrust, pounds

²⁰ Raymond J. Roark, *op. cit.*, p. 134.

²¹ Raymond J. Roark, *op. cit.*, pp. 156-159.

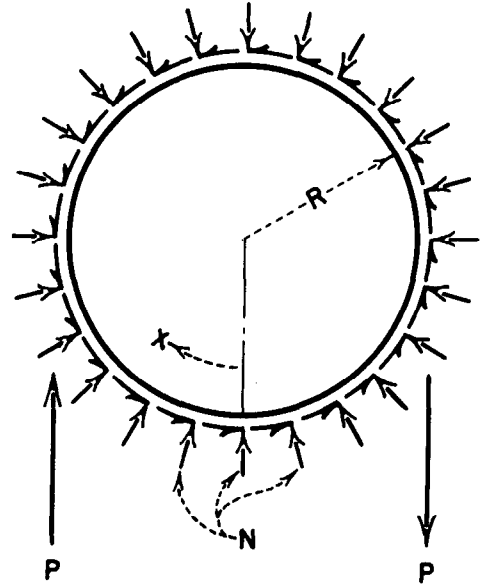


FIGURE 13 - Forces on gate operating ring.

- M = moment in ring from applied load, inch-pounds (see ring solutions)
- c = distance to extreme fiber, inches, positive toward C
- I = moment of inertia of ring cross section, inches⁴
- T₁ = tension in the ring from loads P, pounds
- T₂ = $-\frac{nP}{2\pi}$
- V = shear in ring, pounds
- n = number of wicket gates
- N = radial component of gate link thrust, pounds
- A = cross-sectional area of ring, square inches

The functions of moment and tension shown in Figure 14 should be investigated to determine the location of the maximum stress.

Wicket Gate Linkage

A typical gate linkage is composed of the link pin, the gate link, the gate lever, the shear lever and the shear pin. Occasionally, a breaking link may be used in lieu of the shear pin.

When the shear pin breaking load is applied to the gate linkage, the allowable stress in the affected parts is two-thirds of the yield stress of the material. A breaking load of the shear pin of approximately 2-1/2 times the normal operating load is considered adequate to prevent

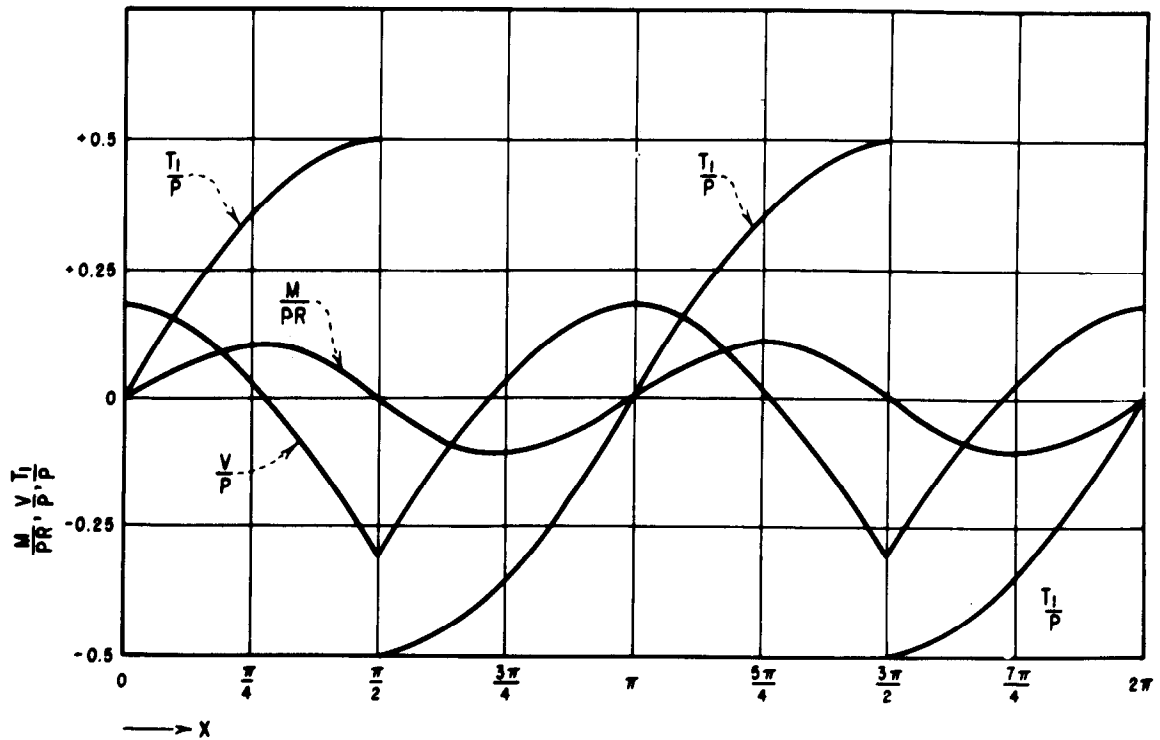
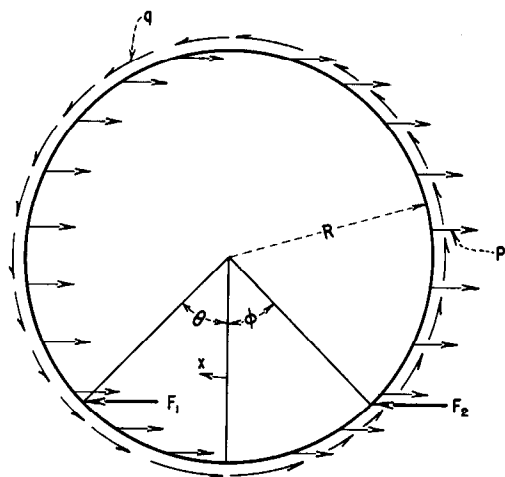


FIGURE 14 - Functions of Moment, Shear, and Tension for ring solution shown in Figure 13.



$$\begin{aligned}
 F_1 + F_2 &= 2\pi R p \\
 F_1 R \cos \theta + F_2 R \cos \phi &= 2\pi q R^2 \\
 M &= M_1 & 0 < x < \theta \\
 M &= M_1 + F_1 R (\cos \theta - \cos x) & \theta < x < 2\pi - \phi \\
 M &= M_1 + F_1 R (\cos \theta - \cos x) + F_2 R (\cos \phi - \cos x) & 2\pi - \phi < x < 2\pi \\
 M_1 &= \frac{F_1 R}{4\pi} \left[2(\pi + x - \theta + \sin \theta \cos \theta) \cos x - 2(\pi + x - \theta) \cos \theta \right. \\
 &\quad \left. - (3 - 2 \sin^2 \theta) \sin x - 2 \sin \theta \right] \\
 &= \frac{F_2 R}{4\pi} \left[2(\pi - x - \phi + \sin \phi \cos \phi) \cos x - 2(\pi - x - \phi) \cos \phi \right. \\
 &\quad \left. + (3 - 2 \sin^2 \phi) \sin x - 2 \sin \phi \right]
 \end{aligned}$$

FIGURE 15 -- Moments in an operating ring.

progressive failure of the shear pins. Stresses in the gate linkage from the maximum normal operating loads are not to exceed the allowable working stresses.

To determine the maximum normal operating forces imposed on the linkage, the force applied to the operating ring by the servomotors (at the point of servomotor attachment) is divided equally among the number of wicket gate linkages, taking note of the radial location of the link pins. The only time that there are forces of any importance acting on the wicket gates and linkage is when the gates are in a closed position, since in the closed position, the nose of the gate acting against the trailing edge of the adjacent gate causes the linkage to become locked. (See Figure 16.) Then the force on the link is equal to the force applied in the tangential direction to the link pin by the operating ring divided by the cosine

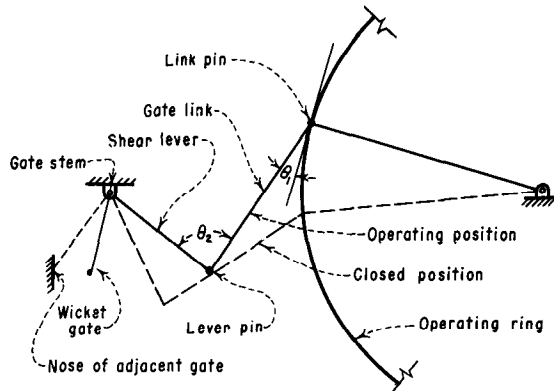


FIGURE 16 - Gate linkage mechanism.

of the angle θ_1 between the link and the tangent to the ring.

It may be noted that as θ_1 approaches 90° , the force on the link in the closed position becomes very large. This is known as "toggle action" and is to be avoided.

With the shear pin stressed to the point of failure, the following items should be checked in the gate linkage mechanism, see Figure 17:

- a. Bending stress in the gate lever
- b. Bending stress in the shear lever
- c. Shear stress in the gate key
- d. Bearing stress in the gate key
- e. Shear tear-out of the linkage pins

- f. Shear on linkage pins, each face
- g. Tension stress in gate link
- h. Column strength of gate link

Wicket Gates

The wicket gates control the flow of water to the turbine.

The maximum combined stress in the wicket gates is limited to two-thirds of the yield point of the material at the breaking strength of the shear pins and cannot exceed the allowable working stress under maximum normal operating conditions.

The maximum normal operating condition is considered to be an equal distribution of the maximum servomotor load to all the gates.

The wicket gate must resist the loads from water pressure (including water hammer) and edge loading caused by operation of the gate linkage (see Figure 18).

Items to be checked in the wicket gate are:

- a. Shear stress in the stem
- b. Bending stress in trailing edge
- c. Bending in gate from water pressure load
- d. Keyway stresses

The nose section of hollow wicket gates may require stiffening diaphragms to prevent high local bending stresses at the juncture of the gate shell and the shaft.

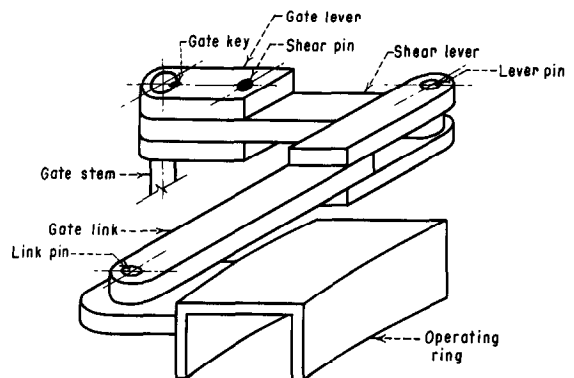
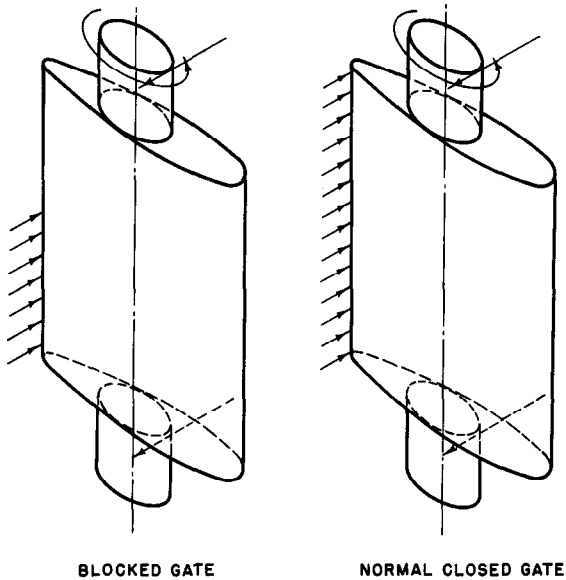


FIGURE 17 - Typical wicket gate linkage system.



BLOCKED GATE

NORMAL CLOSED GATE

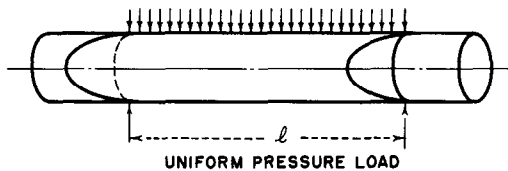


FIGURE 18 - Wicket gate loads.

SPIRAL CASE SUPPORTING STRUCTURE

The spiral case supporting structure consists of the jacks, piers, beams, tie rods, columns, rings, and other equipment necessary to hold the spiral case in position during the concreting process.

Jack Loads

The load carried by the jacks consists of the weight of the spiral case, the water contained within the case, and the vertical components of the tie-rod forces, assuming a tie rod prestress of 10,000 pounds per square inch. The total rated capacity of all the jacks should be 1-1/2 to 2 times the total vertical load.

The portion of the load carried by any one jack can be evaluated by using a plan (to scale) of the spiral case supporting scheme and estimating the region of load carried by each jack.

Tiedown Bars

The tiedown bars are usually assumed prestressed to 10,000 pounds per square inch, through the turnbuckles. All of the connections should withstand this load.

Considering the entire spiral case, either as a whole or as individual parts, the sum of the vertical components of the tie-rod forces should prevent flotation of the water-filled spiral case when it is immersed in grout of specific weight of 100 pounds per cubic foot. Prestressing the tie rods is done to prevent any movement of the spiral case under these conditions.

Jack Pads and Tiedown Lugs

The local circumferential bending stress at the jack pads may be determined from one of the following expressions, whichever is applicable:

when $\frac{b}{R} < 0.05$, use

$$\sigma = \frac{P}{4t} \left[0.42 \ln \left(\frac{0.215R}{b} \right) + \frac{6}{4\pi} \right]^{22}$$

and when $\frac{b}{R} > 0.05$, use

$$\sigma = \frac{P}{2t^2} \ln \left(\frac{0.3R}{b} \right)^{23}$$

where

- P = the radial component of the computed jack load, pounds
- t = the casing shell thickness, inches
- R = the radius of the casing at location of jack, inches
- b = the radius of the loaded area, inches

ln indicates that natural logarithms are to be used.

Usually, the loaded area under the jack pad is nearly rectangular rather than circular. To convert to a circular area, an approximation can be made by using an area equal to the rectangular area and thus obtain a value for b to be used in the above expressions. In this connection, it should be noted that the pads made of angles are not always boxed in with vertical webs on the end. It is suggested in most instances that these vertical webs be added to distribute the load more effectively over

²² Raymond J. Roark, *op. cit.*, Case No. 6, page 270.

²³ Raymond J. Roark, *op. cit.*, page 283.

the area, so that the condition assumed for analysis will be more nearly realized in practice.

The total circumferential stress at the jack pad would then be the bending stress, as calculated above, plus the shell tension stress due to internal pressure. The shell thickness is normally selected to keep the stress due to internal pressure within the allowable design stress given in the specifications. Then it is obvious that adding of the two stresses will give a local stress in excess of that permitted in the specifications as a design stress.

Since this condition exists only locally and since embedment of the spiral case will lessen the loads on the jacks, it is recommended that two-thirds of the yield strength of the material be considered as acceptable for the local stresses at the jack pads.

The tiedown lugs should be checked for their adequacy to develop the forces in the tie bars, allowing comparable values for unit stresses. As an example, the bending stress in the lug (plus tension, if any), should not materially exceed the tension stress in the tie bar which is the source of load.

Support Columns

Columns used in supporting the spiral case should be designed to sustain the rated load of the jack. Many satisfactory column formulas can be found in structural codes, of which the following are typical:

$$\frac{L}{r} \text{ less than } 120, \frac{P}{A} = 17,000 - 0.485 \left(\frac{L}{r} \right)^2$$

$$\frac{L}{r} \text{ greater than } 120, \frac{P}{A} = \frac{18,000}{1 + \frac{L^2}{18,000r^2}}$$

where

- P = total load on the column, pounds
- A = cross-sectional area of column, square inches
- L = unsupported length of column, inches
- r = least radius of gyration of column cross section, inches.

TURBINE RUNNER AND SHAFT

The turbine runner converts the velocity and pressure energy of the water into shaft work.

Turbine Runner or Pump Impeller

Items to be determined for a runner or an impeller are as follows:

a. Ability of the runner to support the superimposed loads during erection, if required. Stresses will usually be low in this case, since dimensional stability requirements of the buckets will provide adequate material where it is needed to carry the load. It should be noted that in the case of the Francis-type runner, shims are usually placed between the band and the draft tube liner for leveling purposes. This will concentrate the load at a few points, causing high bearing stresses.

b. Adequacy of the coupling of runners to the shaft and conformance of the coupling connection with the code of ASA Standard B49.1, 1947.²⁴

c. If a propeller-type runner is used, the bending stress in the blades may be found by considering the blade as a cantilever beam, loaded by forebay pressure acting on the total blade area, causing the blade to bend about its weak axis at the runner hub.

d. It may be possible under certain conditions for forces on the runner to lift the rotating parts of the unit off the thrust bearing.

In a Francis-type unit, uplift may be caused when the horizontal projection of the area between the periphery of the runner and the lower wearing ring exceeds the horizontal projection of the area between the periphery of the runner and the upper wearing ring. This will cause a force to be applied to the unit in the vertical direction owing to the forebay pressure acting on the net annular area. If this force is greater than the weight of the rotating parts plus the hydraulic thrust, the unit may lift off the thrust bearing. Note that in the opposite case, the resulting force will add to

²⁴ ASME, Shaft Couplings—Integrally Forged Flange Type for Hydroelectric Units, ASA Standard B 49.1 1947.

that ascribable to the weight of the unit plus the hydraulic thrust. See Figure 19.

In this type of unit, the radial location of the seal rings may sometimes be changed to eliminate the vertical force. This course is not always possible, and other action must be taken.

In a propeller unit, under conditions of runaway speed, when the wicket gates are closed the water in the draft tube will be depressed by the rapidly moving runner blades. (Sometimes this is artificially done with compressed air, in which case uplift will not be present.) The pressure at the centerline of the runner which is due to the maximum tailwater elevation acting on the cross-sectional area of the draft tube will result in a force acting vertically, Figure 20. If this force exceeds the weight of the rotating parts, uplift of the unit may result.

Uplift of a unit may be remedied by increasing the weight of the rotating parts, by providing a thrust collar to limit the vertical movement of the impeller or runner, or by eliminating the vertical force causing uplift.

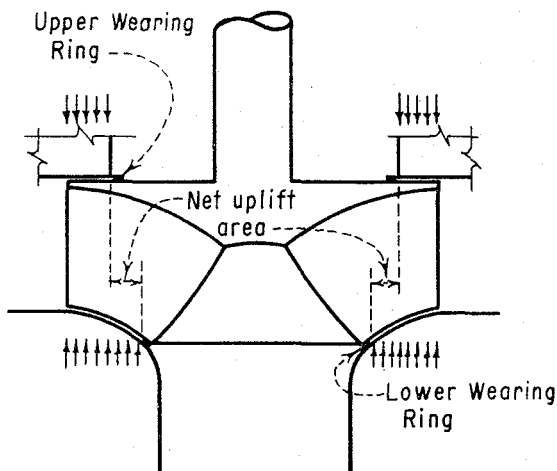


FIGURE 19 - Uplift forces on a Francis turbine.

An increase in the weight of the rotating parts has a generally favorable effect on the operating characteristics of the unit, and is therefore perhaps the most satisfactory solution. Providing a thrust collar to limit the vertical movement presents the difficulty of providing clearance for lifting the unit when starting it, and at the same time limiting the vertical movement while running the unit. The only advantage of such a thrust collar is the prevention of contact of the runner with the head cover.

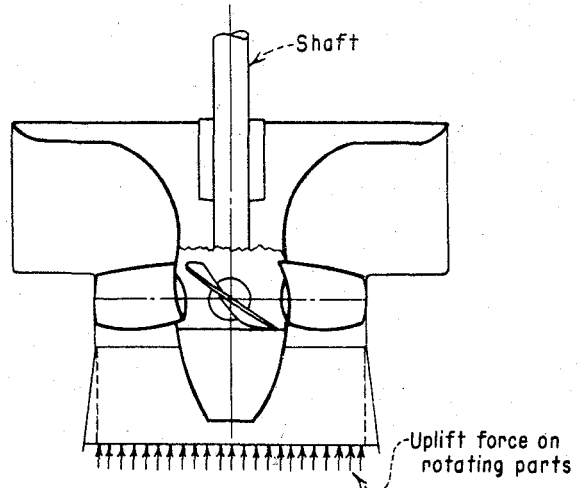


FIGURE 20 - Uplift forces on a propeller turbine.

If the thrust bearing contact is broken, severe damage to the thrust bearing is imminent.

Turbine Shaft

Items to be checked on the turbine shaft are as follows:

- a. Check the shaft couplings with the code of ASA B49.1.²⁵
- b. The design of the shaft should conform to the code of ASA B17c.²⁶
- c. For a Kaplan-type runner, where in the shaft encloses a blade-operating servomotor, the following items should be determined:

(1) Total combined stress at the wall of the shaft servomotor from:

- (a) Runner torque;
- (b) Unbalanced hydraulic thrust;
- (c) Weight of rotating parts; and
- (d) Servomotor pressure.

(2) Stress in the coupling bolts due

²⁵ ASME, *Shaft Couplings--Integrally Forged Flange Type for Hydroelectric Units*, ASA Standard B 49.1 1947.

²⁶ ASME, *Code for Design of Transmission Shafting*, ASA Standard B 17c, 1927 (1947).

TABLE 6 - Computation for critical speed

i	W_i	Δ_i	Δ_i^2	$W_i \Delta_i$	$W_i \Delta_i^2$
1					
2					
3					
4					

to the above effects, including flange action.

(3) Bending stress in flanges of the servomotor may be found by using the procedure as for the spiral case.

d. A critical speed study should be made of the hydroelectric unit of which the turbine shaft is a component. The first critical speed is the speed of rotation of the unit which coincides with the lowest natural frequency of the rotating system in lateral vibration. Operation at this speed must be avoided to prevent the excessive vibration associated with resonance. As a general rule, the first critical speed should be greater than 4/3 of the maximum runaway speed of the unit, or approximately 2 and 1/2 times the normal operating speed.

Timoshenko gives the following formula for the gravest mode of vibration:²⁷

$$f = \frac{1}{2\pi} \sqrt{\frac{g \sum_1^n W_i \Delta_i}{\sum_1^n W_i \Delta_i^2}} \text{ cycles per second,}$$

where Δ_i is the static deflection of the point i on the shaft at the load W_i . This method is approximate, and requires the assumption of a deflection curve of the vibrating shaft. Timoshenko also states that in certain cases the rigidity of the support is low enough to produce a substantial effect on the magnitude of the critical speed. It is only necessary to add to the computed static deflections the displacements caused by the deformation of the supports normal to the centerline of the shaft.

The normal vertical hydroelectric unit may be represented as shown in Figure 21.

²⁷ S. Timoshenko and D. H. Young, *Vibration Problems in Engineering*, 3rd Ed., 1955, page 37.

²⁸ *op. cit.*, page 40.

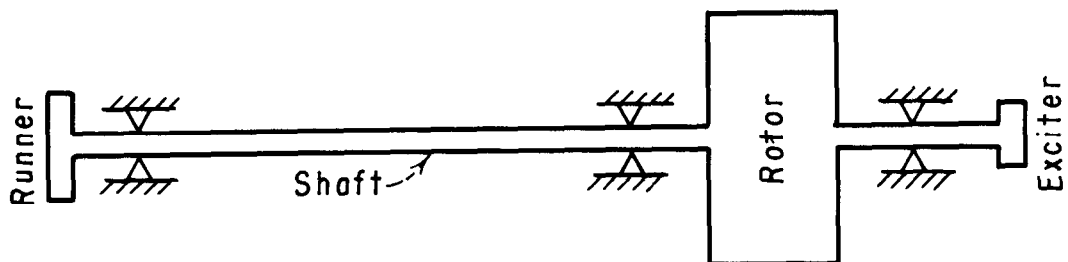


FIGURE 21 - Idealized shaft arrangement.

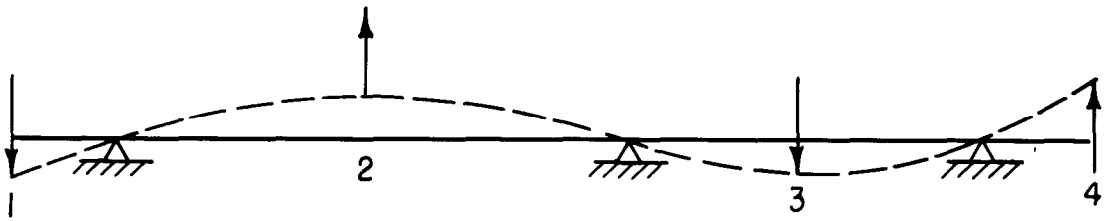


FIGURE 22 - Deflections of shaft from inertia loads.

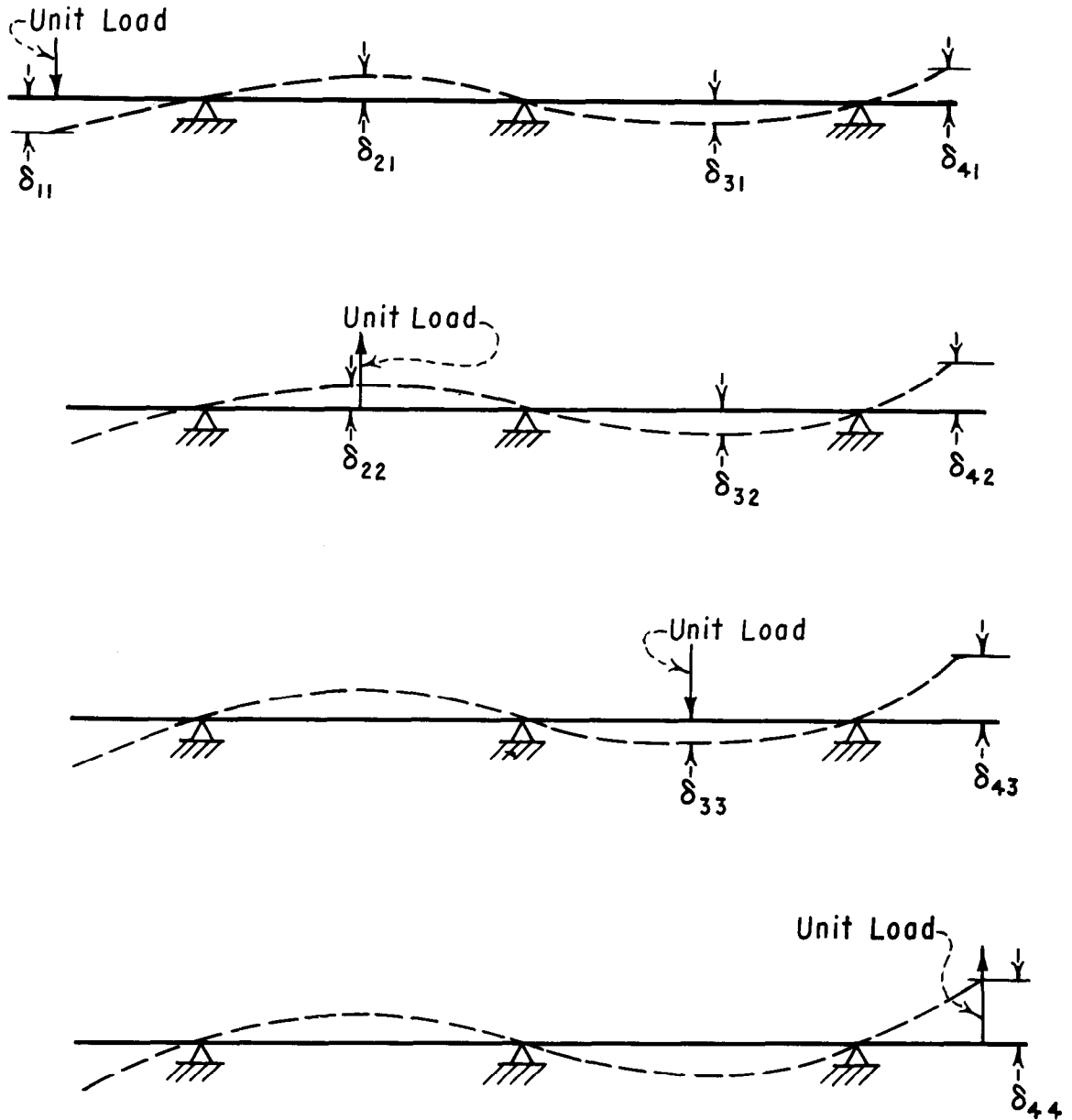


FIGURE 23 - Unit load deflections of shaft.

Figure 22 shows the assumed shape of the deflection curve, and directions of applied loads for the lowest critical speed,

The distributed weight of the shaft may be concentrated as follows:

a. For a cantilever beam, the distributed weight of wl may be concentrated at the end of a cantilever in the amount $\frac{33}{140} wl$

b. For a fixed-ended beam, the distributed weight of wl may be concentrated at the midpoint in the amount $\frac{3}{8} wl$

c. For a beam on simple supports, the distributed load wl may be concentrated at the midpoint in the amount $\frac{1}{2} wl$

Thus the distributed weight of the unit may be broken down into a finite number of concentrated weights.

In evaluating the frequency, the tabular form of Table 6 is suggested. Utilization of Maxwell's laws of reciprocal deflections gives:

$$\Delta_1 = \delta_{11} W_1 + \delta_{12} W_2 + \dots + \delta_{1n} W_n$$

$$\Delta_2 = \delta_{21} W_1 + \delta_{22} W_2 + \dots + \delta_{2n} W_n$$

$$\Delta_n = \delta_{n1} W_1 + \delta_{n2} W_2 + \dots + \delta_{nn} W_n$$

and

$$\delta_{12} = \delta_{21}, \dots, \delta_{m1} = \delta_{1n}$$

To find δ_{11} , δ_{21} , δ_{31} , and δ_{41} (the deflections of Points 1, 2, 3, and 4 due to a unit load at Point 1), the unit is treated as shown in Figure 23. A similar procedure is followed to find δ_{22} , δ_{32} , δ_{42} , δ_{33} , δ_{43} , δ_{44} . Timoshenko gives a typical procedure for this type of calculation.²⁹

The reader is referred to any text on statically indeterminate structures for the procedure to be used in computing deflections of the shaft. It should be noted that removal of one generator guide bearing support will make the problem statically determinate.

²⁹ S. Timoshenko and D. H. Young, *Vibration Problems in Engineering*, 3rd Ed., 1955, pp. 268-281.

GUIDE BEARING SUPPORT BRACKET

The guide bearing support bracket should be designed to resist the maximum loads imposed on it by the turbine shaft and the gate operating ring. Since the bracket takes many forms, only general recommendations will be made regarding its analysis.

The guide bearing support bracket should be of relatively heavy construction to provide rigid support to the turbine guide bearing in both lateral and circumferential directions, as shown in Figure 24. Failure to provide such rigidity may cause a variety of difficulties.

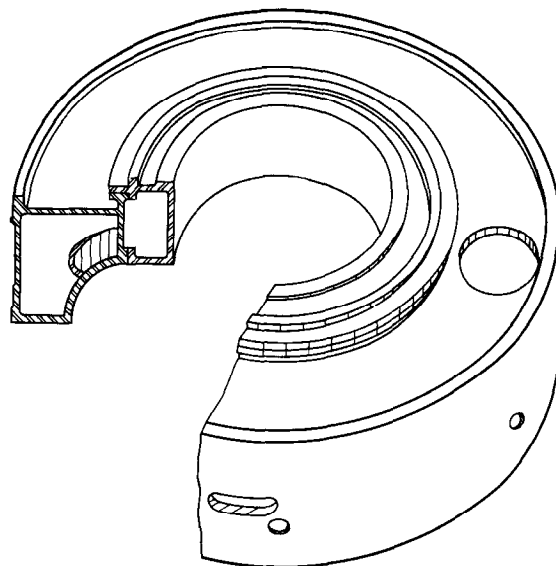
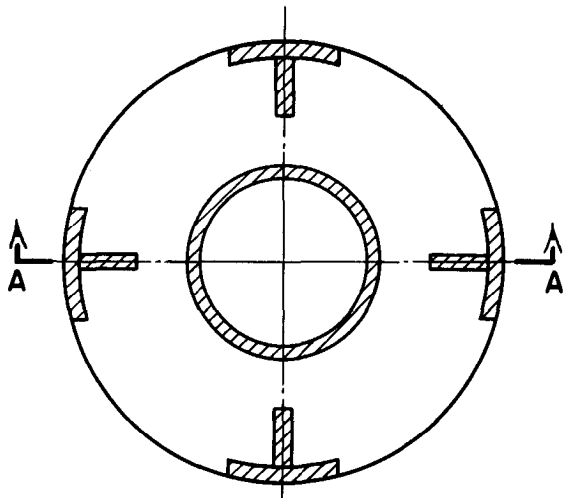


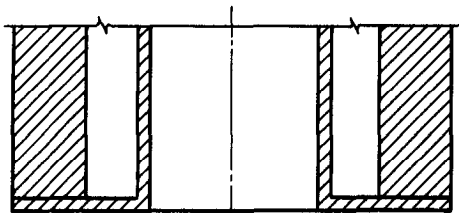
FIGURE 24 - Typical guide bearing bracket.

The load from the shaft may be assumed by considering the rotating parts of the unit as a horizontal beam on simple supports to find the reaction at the turbine guide bearing, Figure 21. To this force is added the unbalanced lateral hydraulic thrust on the runner. Load from the servomotors may be taken as twice the thrust of one servomotor, if the operating ring is carried by the support bracket.

The manner in which the bracket carries the imposed loads depends upon its basic design. Various modes of structural action may be assumed, but the loads are usually carried by shear stress only. Since the vertical ribs which are parallel to the direction of load application offer much more resistance to distortion than those normal to the load, only the components of load parallel to the ribs should be considered.



BEARING SUPPORT BRACKET



SECTION A-A

FIGURE 25 - Guide bearing bracket.

Dowels should be provided between the bracket and the head cover, as described in the section on head covers.

PIT-LINER

The pit-liner serves as an internal form and as a protective liner for the surrounding concrete. The servomotor pistons, lubrication oil systems, access stairways, auxiliary piping, and occasionally the operating ring may be mounted on or in the pit-liner.

The pit-liner may be loaded by the external pressure due to maximum tailwater elevation (in some installations the forebay pressure may be applied), the weight of the superimposed concrete and the unit, and forces due to servomotor operation.

Collapsing Stability

The pit-liner, being well anchored to the surrounding concrete and having circumferential stiffeners, is not likely to collapse. A check may be made using the Saunders and Windenburg formula:³⁰

$$P = 73.4 \times 10^6 \frac{t}{L} \cdot \frac{t}{D} \cdot \left(\frac{t}{D}\right)^{1/2}$$

where

P = collapsing pressure, pounds per square inch

t = thickness of the pipe shell, inches

L = length between circumferential stiffeners, inches

D = diameter of pit-liner, inches

Occasionally a large area of flat plate may be encountered. In this case, the formula, $M = -kqa^2$ on page 25, may be applicable. If not, Roark offers solutions for a wide variety of cases.³¹

Superimposed Loads

The weight of the unit and a portion of the superstructure above the pit-liner may be carried by the pit-liner and transmitted through the stay ring to the foundation. Stresses in the pit-liner may be found for this load by the simple formula:

$$S = \frac{P}{A}$$

where

P = superimposed load, pounds

A = $2\pi r t$

r = radius to middle surface of pit-liner shell, inches

t = thickness of shell, inches

The pit-liner should also be checked for collapsing stability as a thin cylindrical shell subjected to end load. Timoshenko gives the formula:³²

³⁰ Harold E. Saunders and Dwight F. Windenburg, *Strength of Thin Cylindrical Shells Under External Pressure*, 1931, page 209.

³¹ Raymond J. Roark, *op. cit.*, page 192.

³² S. Timoshenko and J. M. Gere, *Theory of Elastic Stability*, 2nd Edition, 1961, page 458.

$$S_{cr} = \frac{Et}{r\sqrt{3(1-\nu^2)}}$$

where

S_{cr} = compressive stress at buckling, pounds per square inch

E = modulus of elasticity of pit-liner material, pounds per square inch

ν = Poisson's ratio

Servomotor Supports

The servomotor recesses of the pit-liner are not ordinarily designed to carry the servomotor load but merely to support the dead weight of the servomotor and transmit the servomotor reaction to the adjacent concrete. This is usually done by putting a large plate of substantial thickness in back of the servomotor to distribute the thrust. To resist the opposite or tensile effect, long rods with plates on the end are usually embedded in the concrete.

The backup plates transmitting the servomotor thrust into the foundation concrete require investigation. These plates may be treated as shown in Timoshenko's example.³³ Figure 26 is a typical example. The maximum stress is

$$\sigma = \frac{Kqa^2}{h^2}, \quad q = \frac{T}{\pi(a^2 - b^2)}$$

where

σ = stress, pounds per square inch

T = servomotor thrust, pounds

t = plate thickness, inches

q = intensity of uniform foundation reaction, pounds per square inch

a = outer radius of plate, inches

b = inner radius of plate, inches

If the pit-liner is designed to carry the load of the servomotor, it may be analyzed as a ring upon which are impressed two equal and opposite forces constituting a

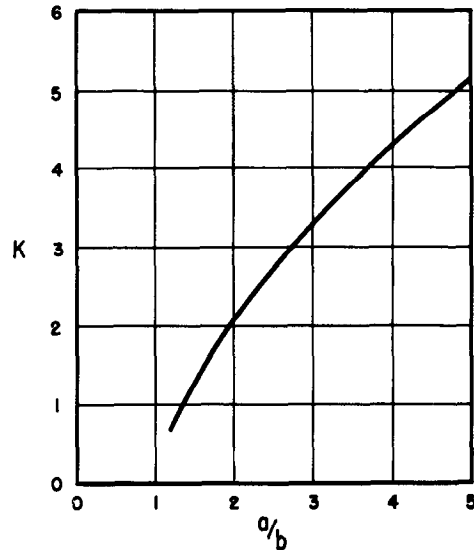
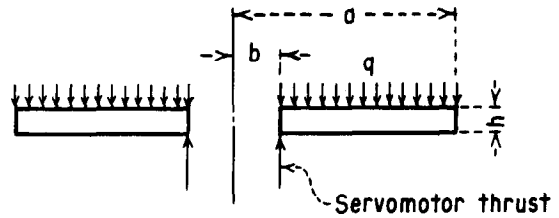


FIGURE 26 - Servomotor thrust plate loading.

couple, the moment of which is resisted by shear forces uniformly distributed around the periphery of the ring. Further cognizance should be taken of the vertical distribution of these forces.

DRAFT TUBE LINER

The draft tube recovers the residual velocity energy of the water leaving the turbine runner. Structurally, the draft tube liner is a relatively unimportant part of a hydraulic turbine installation since it has no primary structural loads to carry. However, it must be capable of withstanding loads caused during erection and loads caused by external hydrostatic pressure during normal operation. Usually, the specifications state that the ribbing and anchorage shall be designed for full external hydrostatic pressure with the tailwater at a specified elevation and with an absolute pressure of one-half atmosphere inside the draft tube liner.

³³S. Timoshenko and S. Woinowsky-Krieger, *Theory of Plates and Shells*, 2nd. Ed., 1961, page 62.

Collapsing Stability

With circumferential ribbing and radial tie rods attached to the ribbing, the circular portion of the draft tube is not likely to collapse. A circular section between ribs may be checked for collapse using the Saunders and Windenburg formula:³⁴

$$P = 73.4 \times 10^8 \frac{t}{L} \cdot \frac{t}{D} \cdot \left(\frac{t}{D} \right)^{1/2}$$

where

P = collapsing pressure, pounds per square inch

t = thickness of the pipe shell, inches

L = length between circumferential ribs, inches

D = diameter of the pipe shell, inches

³⁴ Harold E. Saunders and Dwight F. Windenburg, *op. cit.*, page 209.

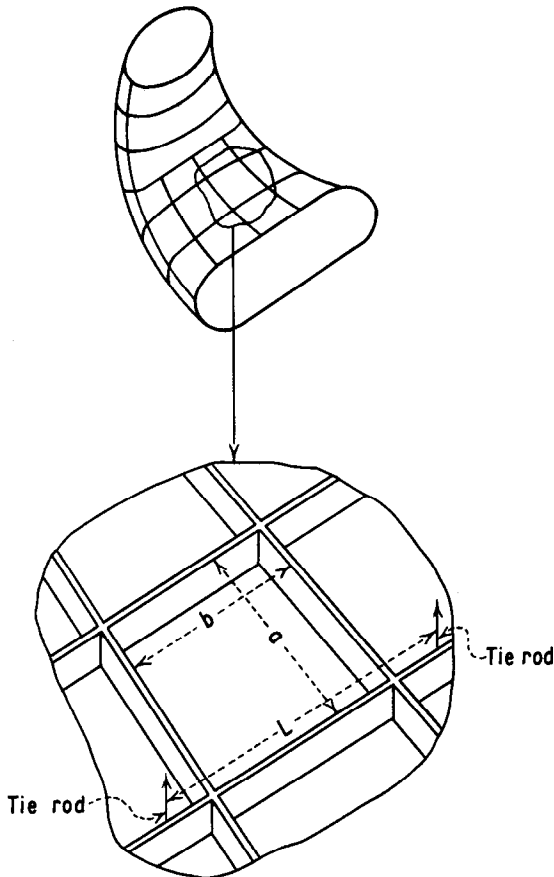


FIGURE 27 - Draft tube liner.

Ordinarily this computed collapsing pressure will be much greater than the design pressure, indicating that collapse of this portion of the draft tube has not been a major factor in its design.

At its downstream end, the draft tube flares out horizontally, creating relatively large, flat sections which must be able to withstand external design pressure. These flat sections of the draft tube should be checked for structural adequacy.

Referring to Figure 27, the plate can be analyzed as a uniformly-loaded, flat, rectangular plate with built-in edges. The maximum stress will occur at the middle of the longer side of the rectangle. The maximum stress is given by:

$$\sigma = \frac{6M}{t^2}$$

where

σ = maximum bending stress, pounds per square inch

M = bending moment at the middle of the long side of the plate, inch-pounds per inch

t = thickness of the plate, inches

The moment M is a function of the lateral dimensions of the plate and the magnitude of the uniform load. M is given by:

$$M = -kqa^2$$

where

k = a constant depending on the dimensions of the plate

q = uniform load, pounds per square inch

a = shorter dimension of the plate, inches

The values of k listed below are taken from Timoshenko:³⁵

where

b = the longer lateral dimension of the plate, inches. For values of b/a greater than 2.0, the value of k is virtually constant at 0.0833.

³⁵S. Timoshenko and S. Woinowsky-Krieger, *Theory of Plates and Shells*, 2nd Ed., 1961, page 202.

b/a	k
1.0	0.0513
1.1	0.0581
1.2	0.0639
1.3	0.0687
1.4	0.0726
1.5	0.0757
1.6	0.0780
1.7	0.0799
1.8	0.0812
1.9	0.0822
2.0	0.0829

Referring again to Figure 27, the section of the draft tube liner between the tie rods at *a* and *b* may be analyzed as a fixed-end beam of length *L*. The beam will consist of the circumferential rib acting as the web of a T-section and a portion of the plate acting as a flange. The width of plate to be included in the effective flange should be $0.181 L$, where *L* is the span of the fixed-end beam.³⁶ The uniform load to be applied to the beam is:

$$w = qa$$

where

w = load per unit length of beam, pounds per inch

q = hydrostatic pressure, pounds per square inch

a = length between circumferential stiffeners, inches

Anchorage

The anchorage rods attached to the flat portions of the draft tube liner should be numerous enough and large enough to support the design hydrostatic load on the liner. To compute the stress in an individual rod, compute the total hydrostatic load on the portion of the liner which the rod will have to support, then divide by the cross-sectional area of the rod.

³⁶ G. Murray Boyd, *Effective Flange Width of Stiffened Plating in Longitudinal Bending*, 1946.

The anchor rods on the draft tube liner, which are oriented so that they exert a downward force on the liner, must be capable of holding the liner in place against the maximum uplift force developed during embedment of the liner in concrete. The numerical value of the uplift force is never known exactly; in fact, the general question is controversial. In the absence of specific data about uplift pressures, a method will be suggested for determining the order of magnitude of the stresses developed in the holddown rods.

Assume the draft tube liner to be immersed in fluid grout of specific weight 100 pounds per cubic foot. Assume the liner to be submerged from its outlet end to the section where it becomes circular. For this portion of the draft tube liner, compute the volume and the weight of the liner. The uplift force is then

$$F = 100 V - W$$

where

V = the computed volume, cubic feet

W = the computed weight, pounds

The area of a holddown rod effective in resisting the uplift force is

$$A_E = A \cos \phi$$

where

A_E = the effective area of the rod, square inches

A = the gross area of the rod cross section, square inches

ϕ = the angle which the rod makes with the vertical

The average tensile stress in the holddown rods is then

$$\sigma = \frac{F}{\Sigma A_E}$$

where ΣA_E is the summation of effective cross-sectional areas of all rods exerting a downward force on the section of draft

MISCELLANEOUS ITEMS

Test Bulkheads

Test ring. -- Normally the test ring used to close the stay ring opening is subjected to high external pressures, and must be checked for its collapsing strength. The stability of the test ring may be provided by stiffener rings or by support points on the ring circumference. In the latter case, a spider may be used, or support bars inserted in the gate stem holes may act as support points for the test ring.

The collapsing pressure of a steel test ring may be determined from the following expression when stiffener rings are used:^{37 38}

$$P = 73.4 \times 10^6 \frac{\left(\frac{t}{D}\right)^{5/2}}{\left(\frac{L}{D}\right)}$$

where

P = collapsing pressure, pounds per square inch

t = test ring shell thickness, inches

³⁷ John Parmakian, *Air-inlet Valves for Steel Pipelines*, 1950.

³⁸ Harold E. Saunders and Dwight F. Windenburg, *op. cit.*, 1931.

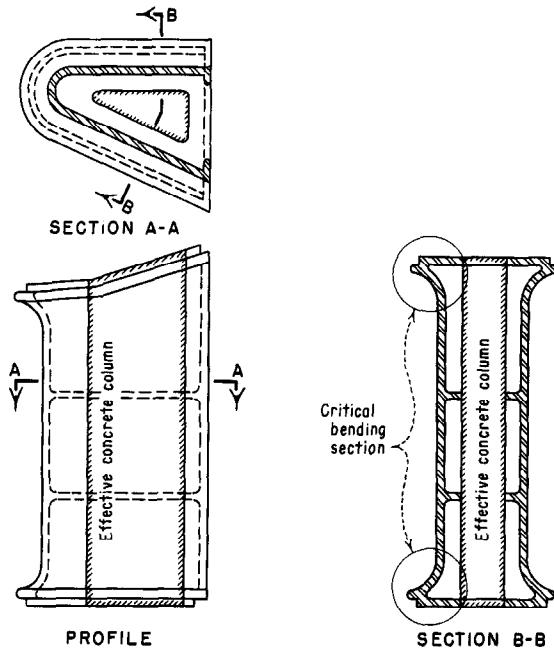


FIGURE 28 - Cast pier nose.

tube liner. This loading on the holddown rods is severe, and judgment must be exercised in interpreting the importance of the computed σ .

Pier Nose

Frequently, the larger draft tubes are designed with multiple outlets which require pier noses where the draft tube splits. These pier noses are usually required to carry large loads which must be transferred from the generator floor to the foundation. Ordinarily, the pier noses are of cast steel and each nose is of special design, requiring a special analysis. The cast pier nose may develop high stresses at the top and bottom where the nose fairs into the concrete of the powerhouse structure. These regions should be checked for bending stresses. If the pier nose is filled with concrete, the concrete will carry a portion of the load as a short column. Only that portion of the concrete which forms a continuous column throughout the length of the pier nose should be used as effective for carrying load. See Figure 28. Figure 29 shows an alternative welded design.

Manhole and Man Door

Owing to the low pressure on the draft tube, the manhole and man door usually are not critical. However, they may be analyzed by the procedure set forth for spiral case manholes and man doors.

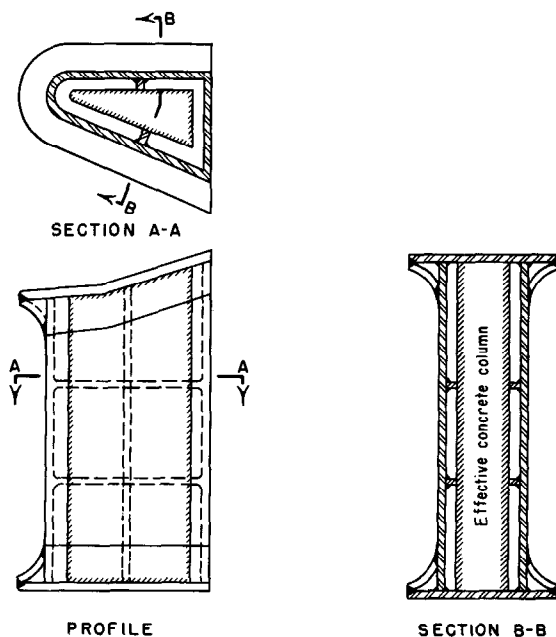


FIGURE 29 - Welded pier nose.

D = outer diameter of test ring, inches

L = spacing between stiffener rings, inches

The stiffened structure may collapse as a whole in which case the collapsing pressure is given by:

$$P = \frac{2 EI(n^2 - 1)}{L' r^2 D}$$

where

E = modulus of elasticity, pounds per square inch

n = minimum number of waves

D = outer diameter of test ring shell, inches

L = spacing between stiffener rings, inches

I = moment of inertia of the cross section of the complete stiffened ring section,³⁹ inches⁴

L' = total height of test ring subjected to external pressure, inches

r = radius to c. g. of the complete stiffened ring section, inches

When the test ring is dependent for its stability upon support points on its circumference, the following equation may be used to determine the collapsing pressure;⁴⁰

$$P = \frac{2 Et^3(n^2 - 1)}{3D^3}$$

where

P = collapsing pressure, pounds per square inch

t = test ring shell thickness, inches

D = diameter of the outer surface of the test ring shell, inches

E = modulus of elasticity of the test ring material, pounds per square inch



FIGURE 30 - Test ring.

n = minimum number of waves into which the shell can buckle

The number of waves is determined by the number of equally spaced points at which the ring is supported. The minimum number of waves is 2. If there are an even number of support points, n is equal to one-half the number of support points. If there are an odd number of support points, n is equal to the number of support points. Figure 30 indicates a test ring having 12 points of support for which n = 6.

External constraint by the stay ring is not considered to assist the test ring in resisting buckling.

Test heads. -- The pressure bulkhead at the inlet to the spiral case may be hemispherical, but this is often not the case. In any event, there have been established certain design criteria for pressure bulkheads which should be observed.⁴¹

Although high local bending stresses may exist near the juncture of the bulkhead and inlet section of the casing, this condition would normally be permissible if the above design criteria are observed. Nevertheless, these bending stresses should be determined, which for hemispherical and ellipsoidal heads can be treated as follows:

Timoshenko gives a discussion of discontinuity stresses when a hemispherical

³⁹ The effective width of shell acting with the stiffener ring may be taken as the ring thickness plus $1.56 \sqrt{rt}$, where r is the radius of the shell in inches, provided the effective widths from adjacent stiffener rings do not overlap, in which case the effective width would extend to midspan between stiffeners. See Reference (9), pages 43-49, for discussion on equivalent flanges.

⁴⁰ S. Timoshenko, *Theory of Elastic Stability*, 1961, page 478.

⁴¹ *Rules for Construction of Unfired Pressure Vessels*, op. cit.

head is used.⁴² The approximate solution of the problem assumes that the bending is of importance only in the zone of the spherical shell close to the joint, and that this zone can be treated as a portion of a long cylindrical shell of the radius of the attached cylinder.

If the thickness of the spherical and the cylindrical portion of the vessel is the same, the moment at the juncture vanishes, leaving only a shear. This shear will induce bending in the shell which when combined with the membrane stress gives (using a hemispherical head),

$$\sigma_{x(\max)} = 1.293 \frac{pr}{2t} \text{ for the maximum longitudinal stress in the cylindrical shell}$$

$$\sigma_{t(\max)} = 1.032 \frac{pr}{t} \text{ for the maximum hoop stress in the cylindrical shell}$$

where

r = radius of cylinder, inches

p = internal pressure, pounds per square inch

t = cylinder wall thickness, inches.

The membrane stress in the hemispherical head is smaller than that in the cylinder, and since the discontinuity stress is the same, the maximum combined stress in the head is always less than that computed above for the cylinder.

When the dished head has the form of an ellipsoid of revolution the discontinuity stresses increase in the proportion of $\frac{r^2}{b^2}$, where r and b are the semimajor and semiminor axes of the ellipse, respectively. The combined stress in the cylindrical shell becomes (with the notation as previously defined):

$$\sigma_{x(\max)} = \left(1 + 0.293 \frac{r^2}{b^2}\right) \frac{pr}{2t}$$

$$\sigma_{t(\max)} = \left(1 + 0.032 \frac{r^2}{b^2}\right) \frac{pr}{t}$$

The above is considered as representative for the stress in the cylindrical shell when the bulkhead is spherically dished (torispherical). Then r and b can be determined as for an ellipsoidal head.

Bottom Ring

The bottom ring may be analyzed as a ring loaded by the uniformly distributed radial forces caused by pressure on the wicket gates. There will be negligible bending present, and the stress is

$$\text{where } S_t = \frac{pr}{A}$$

p = load from wicket gates assumed uniformly distributed over distance between gates, pounds per inch

r = radius to center of wicket gate stems, inches

A = cross-sectional area of bottom ring, square inches.

⁴²S. Timoshenko and S. Woinowsky-Krieger, *Theory of Plates and Shells*, 2nd Ed., 1961, pages 481-485.

LIST OF REFERENCES

- (1) Timoshenko, S., Theory of Plates and Shells, McGraw-Hill Book Company, Inc., New York, Second Ed., 1959
- (2) Cornwell, F. E., Miscellaneous Notes on the General Problem of Flange Design, Bureau of Reclamation, Denver, Colorado
- (3) Roark, Raymond J., Formulas for Stress and Strain, McGraw-Hill Book Company, Inc., New York, Third Ed., 1954
- (4) Timoshenko, S., Strength of Materials, Part II, D. Van Nostrand Company, Inc., New York, Third Ed., 1956
- (5) Timoshenko, S., Theory of Elasticity McGraw-Hill Book Company, Inc., New York, 1951
- (6) Parmakian, John, Air-Inlet Valves for Steel Pipelines, Transactions of American Society of Civil Engineers, v. 115, 1950, page 438
- (7) Timoshenko, S., Theory of Elastic Stability, McGraw-Hill Book Company, Inc., New York, 1961
- (8) Rules for Construction of Unfired Pressure Vessels, Section VIII, ASME Boiler and Pressure Vessel Code, American Society of Mechanical Engineers, New York, 1959
- (9) Penstock Analysis and Stiffener Design, Part V, Bulletin 5, Technical Investigations, Boulder Canyon Project Final Reports, U. S. Department of the Interior, Bureau of Reclamation, Denver, 1940
- (10) Hetenyi, M., Beams on Elastic Foundation, University of Michigan Press, Ann Arbor, 1946
- (11) Timoshenko, S., and Young, D. H., Vibration Problems in Engineering, D. Van Nostrand Company, Inc., New York, Third Ed., 1955
- (12) Saunders, Harold E., and Windenburg, Dwight F., Strength of Thin Cylindrical Shells Under External Pressure, Transactions, American Society of Mechanical Engineers, v. 53, 1931
- (13) Boyd, G. Murray, Effective Flange Width of Stiffened Plating in Longitudinal Bending, Engineering, December 27, 1946
- (14) Evans, W. E., Stress Analysis of a Hydraulic Turbine Stay Ring, Mathematical Report No. 105, U.S. Department of the Interior, Bureau of Reclamation, Denver, November 15, 1954
- (15) Bovet, G. and Th., Contribution to the Stress Analysis of a Tubular Scroll, Information Techniques Charmilles, No. 1, 1945, pages 62-73
- (16) Bovet, Th., Calculation of the Mechanical Strength of Spiral Casing for High Head Turbines, Information Techniques Charmilles, No. 7, 1958
- (17) Hogan, Mervin B., A Survey of Literature Pertaining to Stress Distribution in the Vicinity of a Hole and the Design of Pressure Vessels, v. 41, No. 2, Bulletin No. 48, Utah Engineering Experiment Station, Department of Mechanical Engineering, University of Utah, Salt Lake City, August 1950
- (18) Phillips, H. Boyd, and Allen, Ira E., Stresses Around Rectangular Openings in a Plate, Proceedings of the American Society of Civil Engineers, Journal of Engineering Mechanics Division, v. 86, No. EM3, June 1960
- (19) Dolan, T. J., and McClow, J. H., The Influence of Bolt Tension and Eccentric Loads on the Behavior of a Bolted Joint, Proceedings of the Society for Experimental Stress Analysis, v. VIII, No. 1, 1950, pages 29-43
- (20) Shaft Couplings -- Integrally Forged Flange Type for Hydroelectric Units, American Standards Association, B49.1, 1947, published by the American Society of Mechanical Engineers
- (21) Code for Design of Transmission Shafting, American Standards Association, B17c, 1927, reaffirmed in 1947, sponsored by the American Society of Mechanical Engineers

